

Supporting Information

TiO₂-modified porphyrin-based covalent organic frameworks for efficient catalytic CO₂ conversion to cyclic carbonates

Raveena,^{a,b}, Pratibha Kumari,^{*b}

^a Department of Chemistry, University of Delhi, New Delhi-110007

^bBio-Organic Material Research Laboratory, Department of Chemistry, Deshbandhu College, University of Delhi, Kalkaji, New Delhi-110019, India.

Email: pkumari@db.du.ac.in, pkumarichemistry@gmail.com; ORCID id: 0000-0002-3830-3926

Table of Content

1. Material and Reagents
2. Characterization methods
3. Experimental
 - 3.1 Synthesis of meso-tetra(4-aminophenyl) porphyrin (TAPP)
 - 3.2 Synthesis of meso-tetra(4-aminophenyl) porphyrin cobalt (II) complex (Co-TAPP)
 - 3.3 Synthesis of TiO₂
 - 3.4 Functionalization of TiO₂ (F-TiO₂)
 - 3.5 Synthesis of CoP, CoPTi, and PTi covalent organic frameworks (COFs)
 - 3.6 Application of synthesized COFs in CO₂ cycloaddition reactions with epoxides
 - 3.7 Gram scale reactions
 - 3.8 Reusability experiments

Scheme S1 Synthesis of TAPP

Scheme S2 Metalation of TAPP by cobalt metal ion

Scheme S3 Functionalization of TiO₂ by 4-aminobenzoic acid

Scheme S4 Synthesis of CoP COF by using Co-TAPP, and PDC

Scheme S5 Synthesis of CoPTi COF by using F-TiO₂, Co-TAPP, and PDC

Scheme S6 Synthesis of PTi COF by using F-TiO₂, TAPP, and PDC

Scheme S7 General scheme of CO₂ cycloaddition reaction using epoxide

Figure S1 UV-visible spectra of (A) TAPP, (B) Co-TAPP

Figure S2 Comparative FTIR spectra of (A) TAPP, and (B) Co-TAPP

Figure S3 ^1H NMR spectrum of TAPP

Figure S4 Comparative FTIR spectra of (A) TiO_2 , (B) Functionalized TiO_2 (F- TiO_2), and (C) 4-aminobenzoic acid

Figure S5 Powder-XRD pattern of (A) TiO_2 , and (B) F- TiO_2

Figure S6 (A) TEM image, and (B) SAED pattern of TiO_2

Figure S7 SEM images of F- TiO_2

Figure S8 EDX analysis of F- TiO_2

Figure S9 Comparative FTIR spectra of (A) 2,6-pyridinedicarboxaldehyde (PDC), (B) Co-TAPP, and (C) CoP COF

Figure S10 Comparative FTIR spectra of (A) 2,6-pyridinedicarboxaldehyde (PDC), (B) F- TiO_2 , (C) Co-TAPP, and (D) CoPTi COF

Figure S11 Comparative FTIR spectra of (A) 2,6-pyridinedicarboxaldehyde (PDC), (B) F- TiO_2 , (C) TAPP, and (D) PTi COF

Figure S12 EDX analysis of CoP COF

Figure S13 EDX analysis of CoPTi COF

Figure S14 TGA curve of CoP COF

Figure S15 TGA curve of CoPTi COF

Figure S16 ^1H NMR spectrum of 4-chloromethyl-1,3-dioxolan-3-one (**1b**)

Figure S17 Magnified ^1H NMR spectrum of 4-chloromethyl-1,3-dioxolan-3-one (**1b**)

Figure S18 FTIR spectrum of 4-chloromethyl-1,3-dioxolan-3-one (**1b**)

Figure S19 FTIR spectrum of 4-ethyl-1,3-dioxolan-2-one (**2b**)

Figure S20 ^1H NMR spectrum of 4-ethyl-1,3-dioxolan-2-one (**2b**)

Figure S21 Magnified ^1H NMR spectrum of 4-ethyl-1,3-dioxolan-2-one (**2b**)

Figure S22 FTIR spectrum of 4-[(2-propen-1-yloxy)methyl]-1,3-dioxolan-2-one (**3b**)

Figure S23 ^1H NMR spectrum of 4-[(2-propen-1-yloxy)methyl]-1,3-dioxolan-2-one (**3b**)

Figure S24 Magnified ^1H NMR spectrum of 4-[(2-propen-1-yloxy)methyl]-1,3-dioxolan-2-one (**3b**)

Figure S25 FTIR spectrum of 4-(phenylmethyl)-1,3-dioxolan-2-one (**4b**)

Figure S26 ^1H NMR spectrum of 4-(phenylmethyl)-1,3-dioxolan-2-one (**4b**)

Figure S27 Magnified ^1H NMR spectrum of 4-(phenylmethyl)-1,3-dioxolan-2-one (**4b**)

Figure S28 FTIR spectrum of 4-phenyl-1,3-dioxolan-2-one (**5b**)

Figure S29 ^1H NMR spectrum of 4-phenyl-1,3-dioxolan-2-one (**5b**)

Figure S30 Magnified ^1H NMR spectrum of 4-phenyl-1,3-dioxolan-2-one (**5b**)

Figure S31 FTIR spectrum of 4-(phenoxyethyl)-1,3-dioxolan-2-one (**6b**)

Figure S32 ^1H NMR spectrum of 4-(phenoxyethyl)-1,3-dioxolan-2-one (**6b**)

Figure S33 Magnified ^1H NMR spectrum of 4-(phenoxyethyl)-1,3-dioxolan-2-one (**6b**)

Figure S34 ^1H NMR spectrum of the product for gram scale reaction using epoxide **1a**

Figure S35 ^1H NMR spectrum of the product for gram scale reaction using epoxide **5a**

Figure S36 FTIR spectra of fresh and recovered catalyst of CoPTi COF

Figure S37 Powder-XRD data of fresh and recovered CoPTi COF catalyst

1. Material and Reagents

Every reagent is commercially accessible, of analytical grade quality, and doesn't require additional purification. Pyrrole, and Titanium (IV) isopropoxide (TTIP) were purchased from Indus Chem Bio. Glacial acetic acid was acquired from Avantor. Sodium hydroxide (NaOH), Lactic acid, Butanol, Triethylamine, Methanol, Stannous chloride ($\text{SnCl}_2 \cdot 2\text{H}_2\text{O}$), Dimethylformamide (DMF), and Ethanol was purchased from Changshu Hongsheng Fine Chemical Co. Ltd. Nitrobenzene, 4-Nitrobenzaldehyde, Tetrabutylammonium iodide (TBAI) were acquired from Spectro Chem. Cobalt chloride ($\text{CoCl}_2 \cdot 6\text{H}_2\text{O}$), and Sodium sulphate chemicals were purchased from Merck. 2,6-Pyridinedicarboxaldehyde (PDC), 2,3-Epoxypropylphenyl ether, 2,3-Epoxypropyl benzene were acquired from Sigma Aldrich. 1,2-Dichlorobenzene (DCB), Tetrabutylammonium bromide (TBAB), and 4-Amino benzoic acid were acquired from Loba Chemie Pvt. Ltd. Epichlorohydrin was purchased from Thermo

Scientific. Allyl glycidyl ether, Epoxybutane, and Styrene oxide were purchased from Tokyo Chemical Industry Co Ltd.

2. Characterization methods

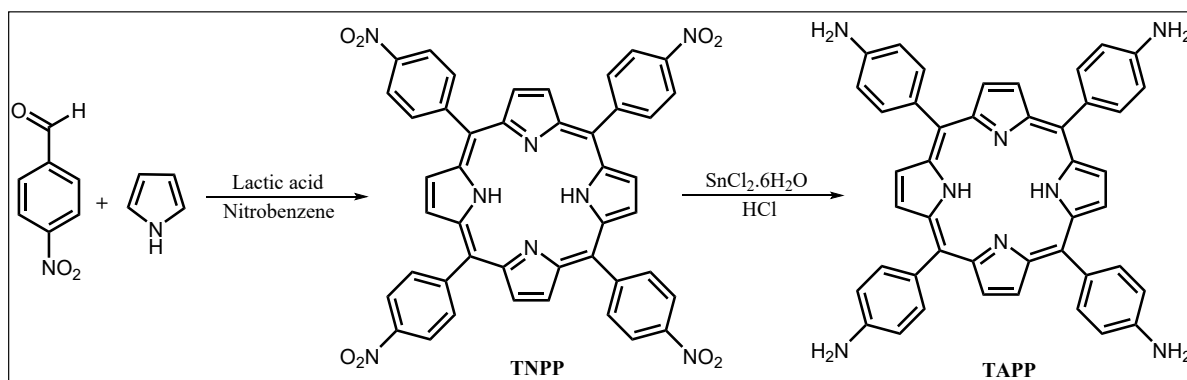
The FTIR spectra were recorded by Nicolet iS50 FTIR Tri-detector instrument using the ATR method from 4000-400 cm^{-1} . The powder-XRD spectra were recorded on Table Top X-ray Diffractometer: Malvern Panalytical, Aeris using Cu X-ray source at 300 W. ^1H NMR spectra were recorded on Jeol, Model: JNM-ECZ 400S (400 MHz). TEM images and SEM images accompanied with EDX on Tecnai G2 20 S-TWIN [FEI] at 20 Kv, and JEOL Japan Mode: JSM 6610LV respectively. The thermal stability of the compound was measured by Thermo Gravimetric Analysis (TGA) curve using TGA HiRes 1000 RT to 1100C. UV-visible spectra were recorded on the Shimadzu UV-Visible 1900 series. Surface area, pore size, and CO_2 uptake ability were obtained by Brunauer-Emmett-Teller Surface area analyzer: Constant volume gas adsorption method + AF5MTM. The element-binding energy and oxidation states were determined by X-ray photoelectron spectrum using the Thermofisher scientific (Model: Nexsa) instrument.

3. Experimental

3.1 Synthesis of meso-tetra(4-aminophenyl) porphyrin (TAPP)

The TAPP was prepared by the reduction of *meso*-tetra(4-nitrophenyl) porphyrin (TNPP) as per the reported method.¹

UV/Vis (methanol): λ_{max} (nm) = 424 (Soret) and 519, 563, 657, 717 (Q band). FTIR (ATR, cm^{-1}): ν = 3342 (w), 2914 (w), 2854 (w), 1596 (s), 1506 (w), 1460 (s), 1344 (w), 1279 (s), 1227 (w), 1162 (s), 962 (m), 793 (s), 728 (s). ^1H NMR (DMSO- d_6 , 400 MHz): δ (ppm) = -2.74 (2H, s, inner -NH of pyrrole), 5.56 (bs, 8H, Ph-NH₂), 7.00 (d, 3J = 8.2 Hz, 8H, ArH, ortho), 7.85 (d, 3J = 8.2 Hz, 8H, ArH, meta), 8.88 (bs, 8H, β -pyrrolic proton).

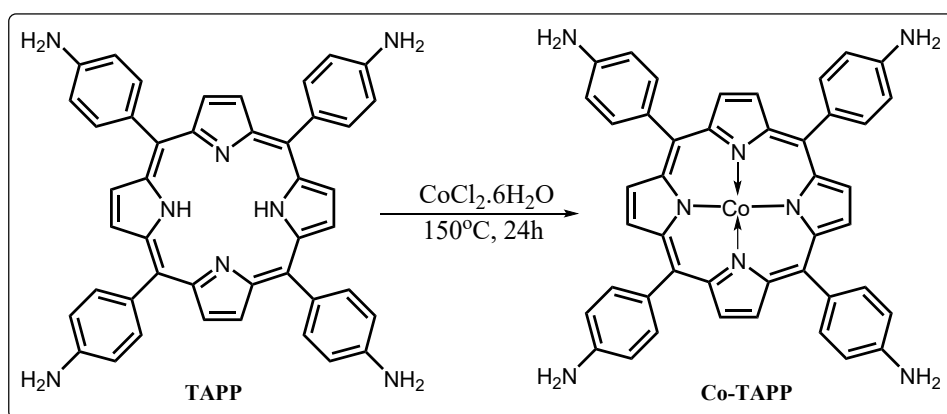


Scheme S1 Synthesis of TAPP

3.2 Synthesis of meso-tetra(4-aminophenyl) porphyrin cobalt (II) complex (Co-TAPP)

The metalation of TAPP was carried out by slight modification in the earlier described method.² TAPP (0.5 gm, 0.74 mmol) was dissolved in 200 mL of DMF. The resulting solution was then refluxed at 150°C with stirring for 1 hour. Subsequently, $\text{CoCl}_2 \cdot 6\text{H}_2\text{O}$ (2.4 gm, 9.99 mmol) was added in small portions to the reaction mixture. The mixture was then refluxed for 24 hours with stirring. Following this, TLC confirmed the absence of free base TAPP in the reaction mixture. The reaction mixture was then cooled, and 150 mL of water was added. The solid product was obtained through centrifugation at 5000 rpm for 8 minutes, washed with acetone, and dried at 70°C for 24 hours.

UV/Vis (methanol): λ_{max} (nm) = 445 (Soret), and 554, 596 (Q band). FTIR (ATR, cm^{-1}): ν = 3343 (w), 2922 (m), 2857 (m), 1651 (s), 1607 (w), 1379 (s), 1172 (m), 1088 (m), 996 (m), 942 (w), 793 (m).



Scheme S2 Metalation of TAPP by cobalt metal ion

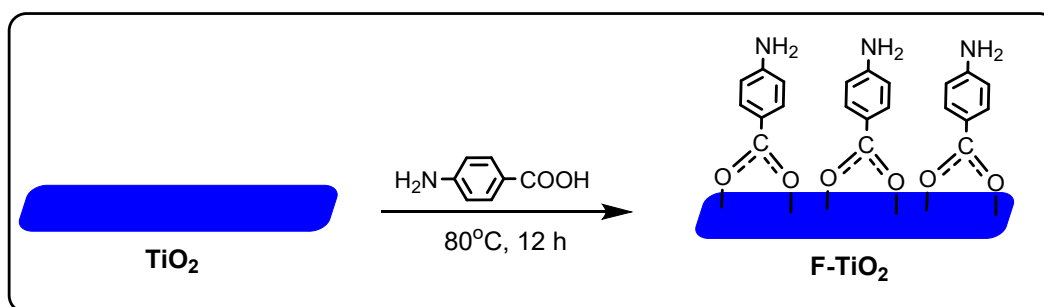
3.3 Synthesis of Titanium dioxide (TiO_2)

The TiO_2 was synthesized by a slight modification in the earlier reported procedure.³ In a 100 mL one-neck round bottom (RB) flask, 40 mL of cold distilled water was placed, and the flask was then stirred at 20°C. A single addition of 4 mL of TTIP was made, after which the RB flask was covered with a lid, resulting in the appearance of a white solution that was stirred for 30 minutes. Following this, 9 mL of glacial acetic acid was added, and the solution was left to stir constantly for 3 hours at 80°C. The heating was then turned off, and the solution was allowed to cool with continuous stirring. Upon cooling, the suspended particles were precipitated by adjusting the pH of the suspension with 10 mL of concentrated 10M NaOH

solution. The precipitated particles were centrifuged and washed with distilled water until reaching a pH of 7. Finally, the TiO_2 sludge was dried in an oven at 100°C for 24 hours. The dried powders were then ground and homogenized in a mortar.

3.4 Functionalization of TiO_2 (F- TiO_2)

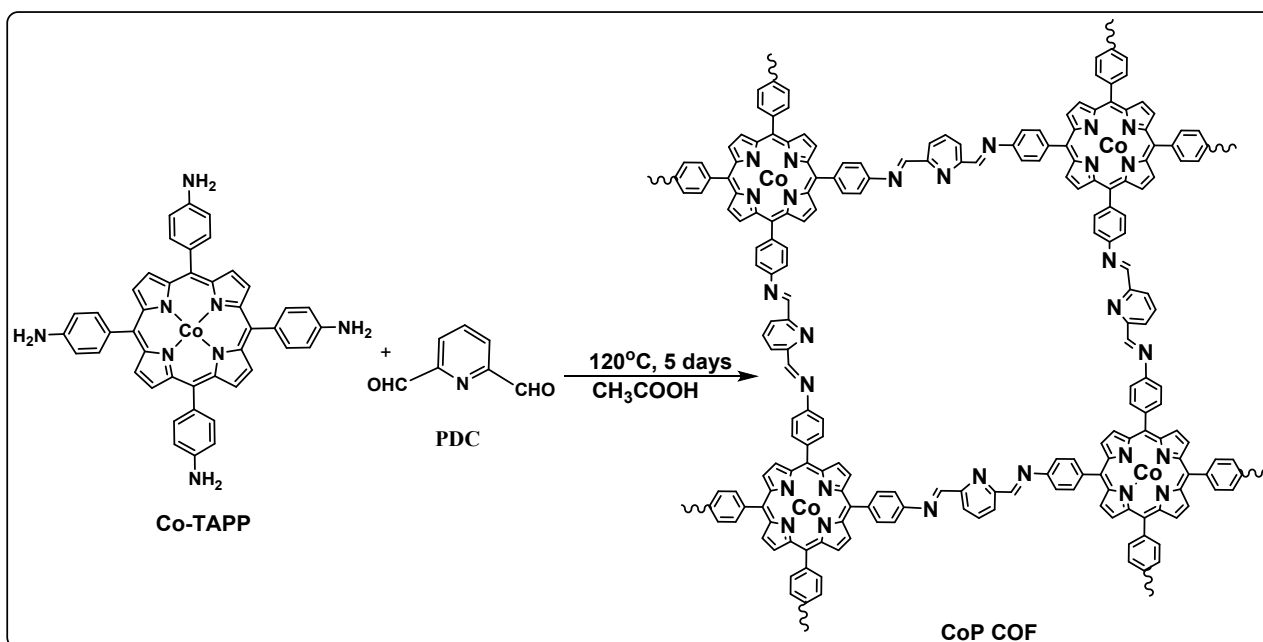
TiO_2 was functionalized by 4-aminobenzoic acid by slightly altering the previously described method.⁴ Initially, 1.25 mmol (0.5 g) of TiO_2 was dispersed in 200 mL of ethanol in a 250 mL two-neck RB flask. Subsequently, 25 mmol (3.4 gm) of 4-aminobenzoic acid was added in small portions to the RB flask. Following this, 5 mL of triethylamine was introduced into the RB flask under stirring conditions. The resulting solution was then refluxed at 80°C for 12 hours. Afterward, the solution was cooled and centrifuged, and the solid compound was washed with ethanol and chloroform to eliminate unreacted components. Finally, the compound was dried at 50°C in an oven for 12 hours.



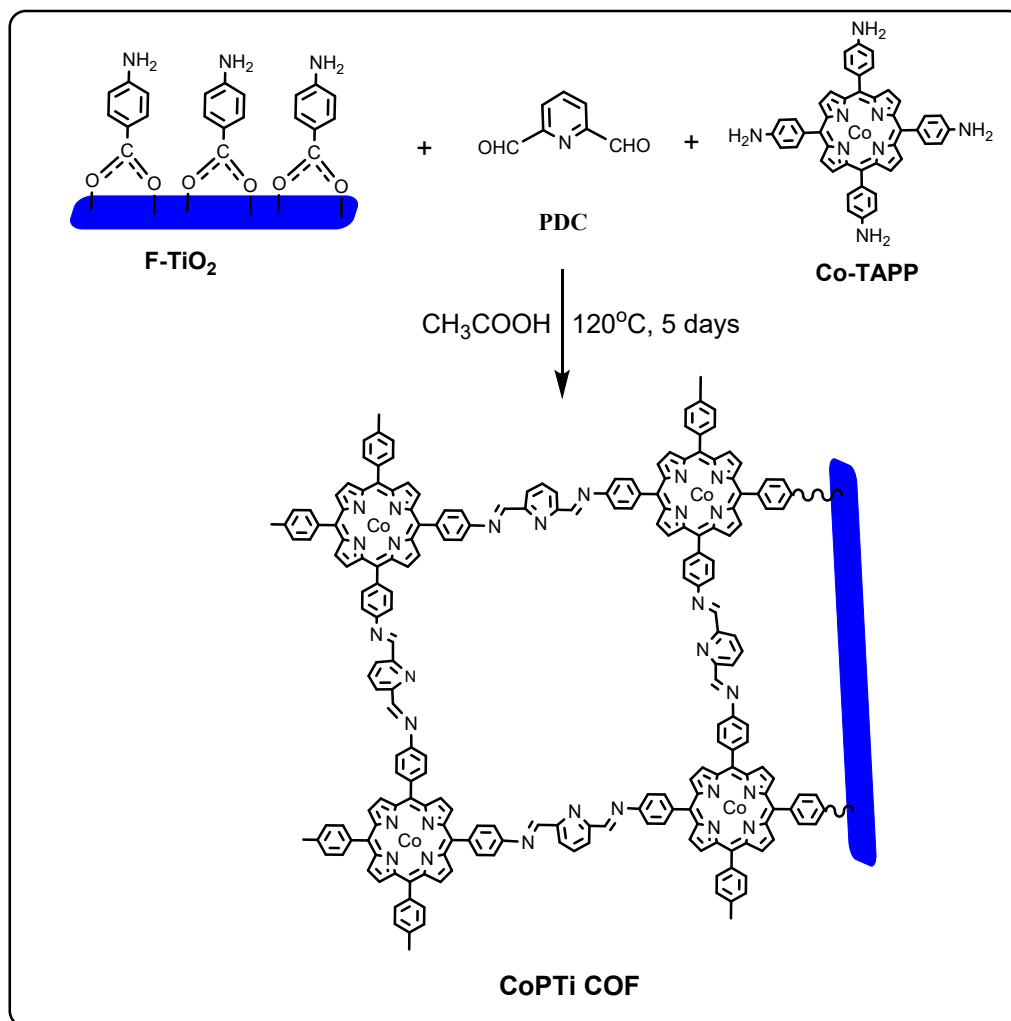
Scheme S3 Functionalization of TiO_2 by 4-aminobenzoic acid

3.5 Synthesis of CoP, CoPTi COF and PTi COF

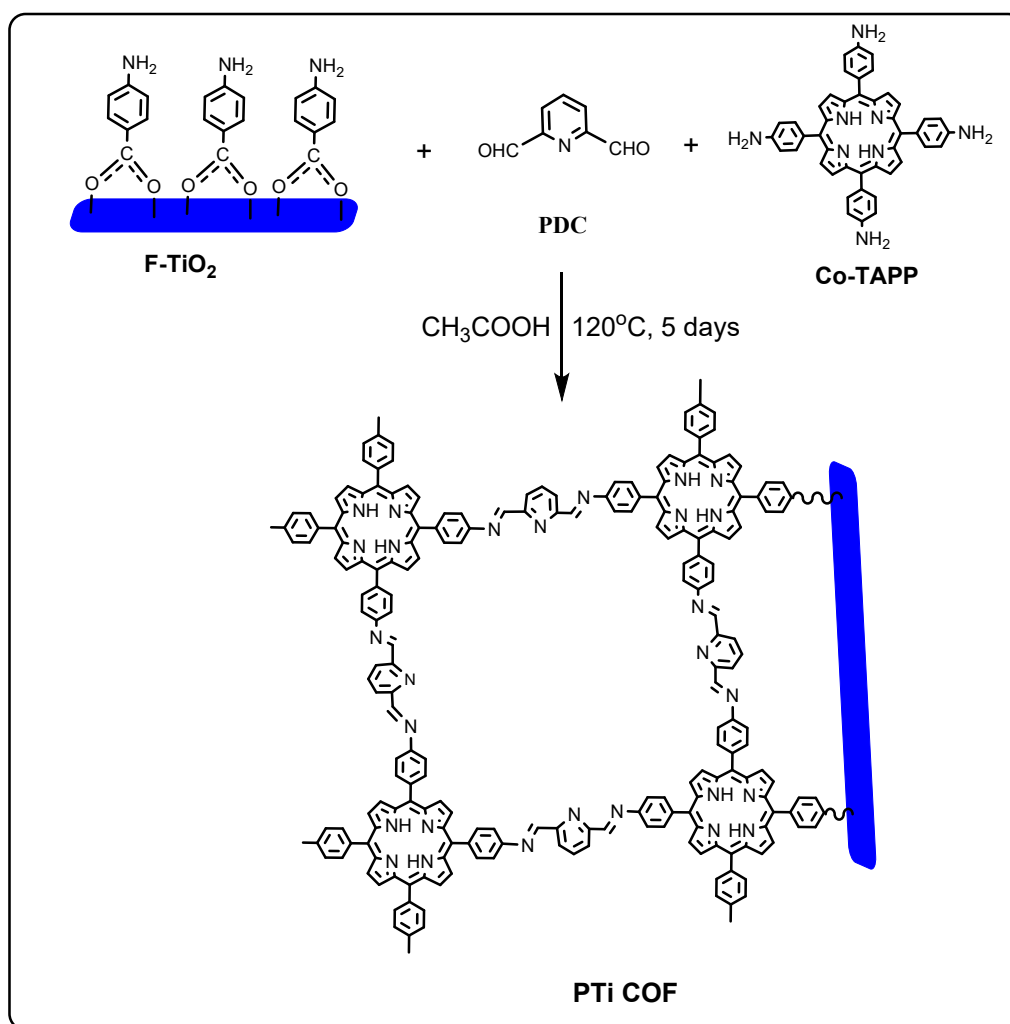
The process of linking aldehyde and amino functional groups was carried out using the reported method.⁵ For the synthesis of CoP COF, Co-TAPP (0.14 mmol) and 2,6-pyridine dicarboxaldehyde (PDC) (0.54 mmol) were used in the condensation reaction. To synthesize CoPTi COF, Co-TAPP (0.14 mmol), PDC (0.84 mmol), and F- TiO_2 (0.07 mmol) were utilized. For the formation of PTi COF, TAPP (0.14 mmol), PDC (0.84 mmol), and F- TiO_2 (0.07 mmol) were taken in a 50 ml RB flask. Following this, 2.5 ml of 1,2-dichlorobenzene (DCB) and 2.5 ml of butanol were added to the mixture. The reactants were homogenized using sonication, after which 700 μL of 6M glacial acetic acid was added. The resulting solution was refluxed at 120°C for 5 days. Subsequently, the reaction mixture was centrifuged at 10000 rpm for 5 minutes and washed seven times with DMF, THF, and acetone. The resulting solid product was obtained and dried at 30°C for 12 hours.



Scheme S4 Synthesis of CoP COF by using Co-TAPP, and PDC



Scheme S5 Synthesis of CoPTi COF by using F-TiO₂, Co-TAPP, and PDC

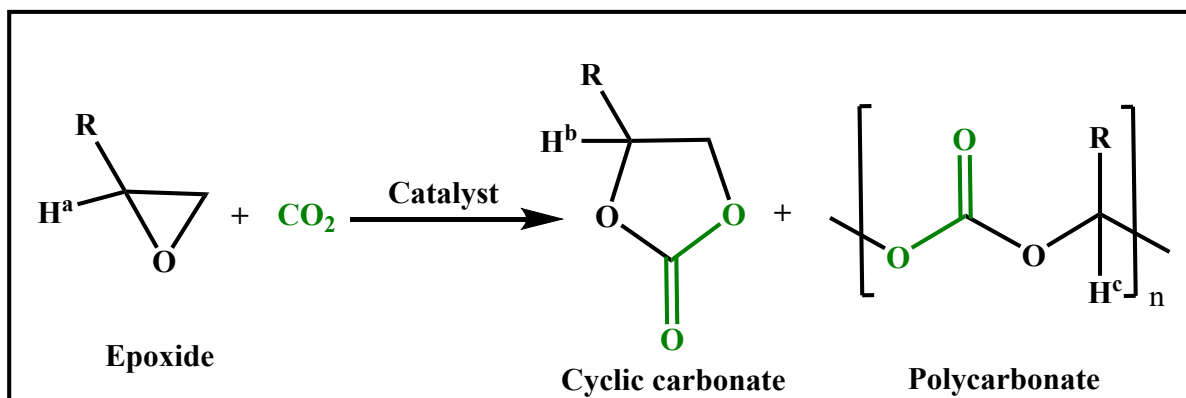


Scheme S6 Synthesis of PTi COF by using F-TiO₂, TAPP, and PDC

3.6 Application of synthesized COF in CO₂ cycloaddition reaction

3.6.1 General procedure

The epoxide (38.9 mmol), catalyst CoPTi COF, and co-catalyst TBAB were taken in a glass vial sealed with Teflon. The CO₂ was inserted by the balloon and then placed at the desired temperature. The reaction was stirred for 24 hours. Thereafter, chloroform was added to the reaction mixture to separate the catalyst and product. Then, the reaction mixture was centrifuged and the product was present in the supernatant, it was dried and the ¹H NMR spectrum was recorded in CDCl₃. The solid catalyst was obtained and it was washed with chloroform 5 times, after that it was dried at 40°C and reused. The percentage selectivity, percentage conversion, and percentage yield of polycarbonate and cyclic carbonate were determined by ¹H NMR spectrum applying the given equations 1-4.⁶⁻¹¹



Scheme S7 General scheme of CO₂ cycloaddition reaction using epoxide

$$\% \text{ conversion of the epoxide into product} = \frac{H_b + H_c}{H_a + H_b + H_c} \times 100$$

(1)

$$\% \text{ yield of cyclic carbonate} = \frac{H_b}{H_a + H_b + H_c} \times 100$$

(2)

$$\% \text{ yield of polycarbonate} = \frac{H_c}{H_a + H_b + H_c} \times 100$$

(3)

$$\% \text{ Selectivity of cyclic carbonate} = \frac{\% \text{ yield of cyclic carbonate}}{\% \text{ conversion}} \times 100$$

(4)

The products were purified by column chromatography and were characterized by FTIR and ¹H NMR spectra.

4-chloromethyl-1,3-dioxolan-3-one (**1b**)^{12,13}

FTIR (ATR, cm⁻¹): ν = 2919 (w), 2853 (w), 1780 (s), 1392 (m), 1162 (s), 1063 (s), 764 (s), 717 (m), 660 (m). ¹H NMR (400 MHz, CDCl₃): δ (ppm) = 4.93 (dddd, ³J = 8.5 Hz, ³J = 5.7 Hz, ³J = 5.4 Hz, ³J = 3.7 Hz, 1H, -CO-O-CH-), 4.54 (dd, ²J = 8.8 Hz, ³J = 8.5 Hz, 1H, -CO-O-CH₂-), 4.35 (dd, ²J = 8.8 Hz, ³J = 5.7 Hz, 1H, -CO-O-CH₂-), 3.74 (dd, ²J = 12.2 Hz, ³J = 5.4 Hz, 1H, -CH₂Cl), 3.67 (dd, ²J = 12.2 Hz, ³J = 3.7 Hz, 1H, -CH₂Cl).

4-ethyl-1,3-dioxolan-2-one (**2b**)¹²

FTIR (ATR, cm^{-1}): $\nu = 2919$ (s), 2850 (w), 1785 (s), 1458 (m), 1374 (m), 1253 (m), 1175 (m), 1055 (s), 786 (m), 704 (w). ^1H NMR (400 MHz, CDCl_3): δ (ppm) = 4.59 (dddd, $^3J = 8.2$ Hz, $^3J = 7.0$ Hz, $^3J = 5.8$ Hz, $^3J = 5.76$ Hz, 1H, -CO-O-CH), 4.46 (dd, $^2J = 8.7$ Hz, $^3J = 8.2$ Hz, 1H, -CO-O-CH₂), 4.02 (dd, $^2J = 8.7$ Hz, $^3J = 7.0$ Hz, 1H, -CO-O-CH₂), 1.82-1.63 (m, 2H, -CH₂-CH₃), 0.97 (t, $^3J = 7.4$ Hz, 3H, -CH₂-CH₃).

4-[(2-propen-1-yloxy)methyl]-1,3-dioxolan-2-one (3b)^{12,13}

FTIR (ATR, cm^{-1}): 2989 (w), 2925 (w), 2866 (w), 1786 (s), 1398 (w), 1393(m), 1159 (s), 1040 (s), 924 (m), 773 (m), 714 (m). ^1H NMR (400 MHz, CDCl_3): δ (ppm) = 5.80 (ddt, $^3J = 17.2$ Hz, $^3J = 10.4$ Hz, $^3J = 5.6$ Hz, 1H, CH₂=CH-), 5.22 (ddt, $^3J = 17.2$ Hz, $^2J = 1.6$ Hz, $^4J = 1.6$ Hz, 1H, CH₂=CH-, trans), 5.15 (ddt, $^3J = 10.4$ Hz, $^2J = 1.6$ Hz, $^4J = 1.2$ Hz, 1H, CH₂=CH-, cis), 4.77 (dddd, $^3J = 8.4$ Hz, $^3J = 6.0$ Hz, $^3J = 3.8$ Hz, $^3J = 3.76$ Hz, 1H, -CO-O-CH-), 4.44 (dd, $^2J = 8.4$ Hz, $^3J = 8.4$ Hz, 1H, -CO-O-CH₂-), 4.33 (dd, $^2J = 8.4$ Hz, $^3J = 6.0$ Hz, 1H, -CO-O-CH₂-), 4.00-3.96 (m, 2H, CH₂=CH-CH₂-), 3.63 (dd, $^2J_{\text{dc}} = 11.2$ Hz, $^3J_{\text{dc}} = 3.8$ Hz, 1H, CH₂=CH-CH₂-O-CH₂-), 3.55 (dd, $^2J = 11.2$ Hz, $^3J = 3.76$ Hz, 1H, CH₂=CH-CH₂-O-CH₂-).

4-(phenylmethyl)-1,3-dioxolan-2-one (4b)¹⁴

FTIR (ATR, cm^{-1}): $\nu = 3029$ (w), 2923 (w), 2855 (w), 1786 (s), 1163 (s), 1053 (s), 761 (m), 702 (s). ^1H NMR (400 MHz, CDCl_3): δ (ppm) = 7.28-7.13 (m, 5H, ArH), 4.84 (dddd, $^3J = 8.0$ Hz, $^3J = 6.9$ Hz, $^3J = 6.4$ Hz, $^3J = 6.4$ Hz, 1H, -CO-O-CH-), 4.34 (dd, $^2J = 9.2$ Hz, $^3J = 8.0$ Hz, 1H, -CO-O-CH₂-), 4.07 (dd, $^2J = 9.2$ Hz, $^3J = 6.9$ Hz, 1H, -CO-O-CH₂-), 3.05 (dd, $^2J = 14.4$ Hz, $^3J = 6.4$ Hz, 1H, Ph-CH₂-), 2.90 (dd, $^2J = 14.4$ Hz, $^3J = 6.4$ Hz, 1H, Ph-CH₂-).

4-phenyl-1,3-dioxolan-2-one (5b)^{12,13}

FTIR (ATR, cm^{-1}): $\nu = 3461$ (br), 2922 (w), 1782 (s), 1165 (s), 1063 (s), 761 (m), 695 (s). ^1H NMR (400 MHz, CDCl_3): δ (ppm) = 7.38-7.27 (m, 5H, ArH), 5.60 (t, $^3J = 8.0$ Hz, 1H, -CO-O-CH-), 4.72 (dd, $^2J = 9.2$ Hz, $^3J = 8.0$ Hz, 1H, -CO-O-CH₂-), 4.26 (dd, $^2J = 9.2$ Hz, $^3J = 8.0$ Hz, 1H, -CO-O-CH₂-).

4-(phenoxyethyl)-1,3-dioxolan-2-one (6b)^{12,13}

FTIR (ATR, cm^{-1}): $\nu = 2921$ (m), 2852 (m), 1788 (m), 1597 (m), 1493 (m), 1254 (s), 1162 (s), 1081 (s), 751 (s), 693 (s). ^1H NMR (400 MHz, CDCl_3): δ (ppm) = 7.25-6.82 (m, 5H, ArH), 4.95 (dddd, $^3J = 8.5$ Hz, $^3J = 6.0$ Hz, $^3J = 4.2$ Hz, $^3J = 3.6$ Hz, 1H, -CO-O-CH), 4.53 (dd, $^2J = 9.0$ Hz, $^3J = 8.5$ Hz, 1H, -CO-O-CH₂-), 4.46 (dd, $^2J = 9.0$ Hz, $^3J = 6.0$ Hz, 1H, -CO-O-CH₂-), 4.16

(dd, $^2J= 10.8$ Hz, $^3J= 4.2$ Hz, 1H , Ph-O-CH₂-), 4.06 (dd, $^2J= 10.8$ Hz, $^3J= 3.6$ Hz, 1H, Ph-O-CH₂-).

3.7 Reusability experiment

Reusability is an important parameter of practical applications. The catalyst CoPTi COF (20 mg), epoxide (**1a**, 7.78 mmol), TBAB (0.006 mmol), 80°C, 24 hours stirring. After completing the reaction, the catalyst and product were separated using chloroform. The percentage yield and selectivity of cyclic carbonate were calculated by equation 1-4 using ^1H NMR of the reaction mixture. The catalyst was recovered by washing it with chloroform five times and drying it at 40°C in an incubator. After that, the catalyst was reused for the next cycle. This process was repeated three times.

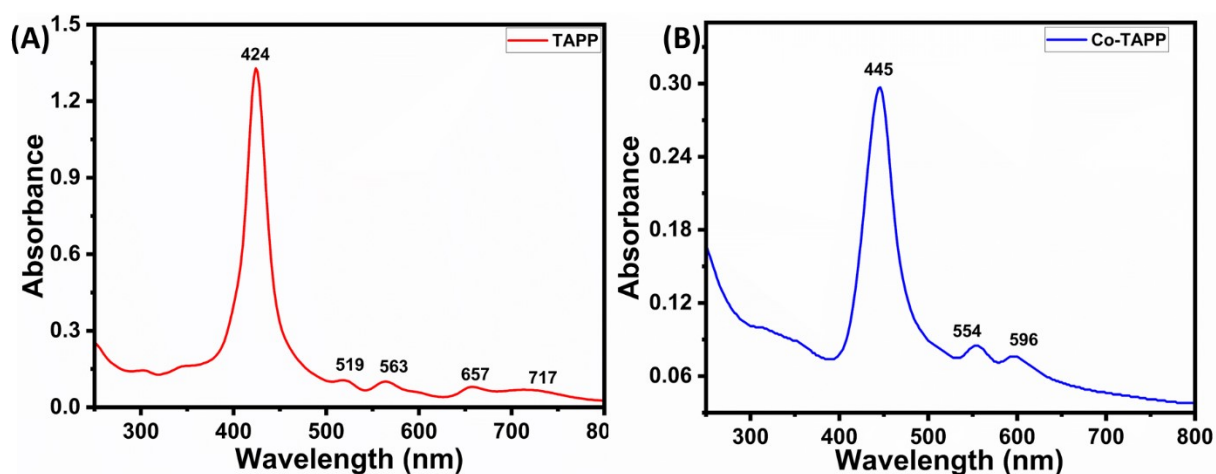


Figure S1 UV-visible spectra of (A) TAPP, (B) Co-TAPP

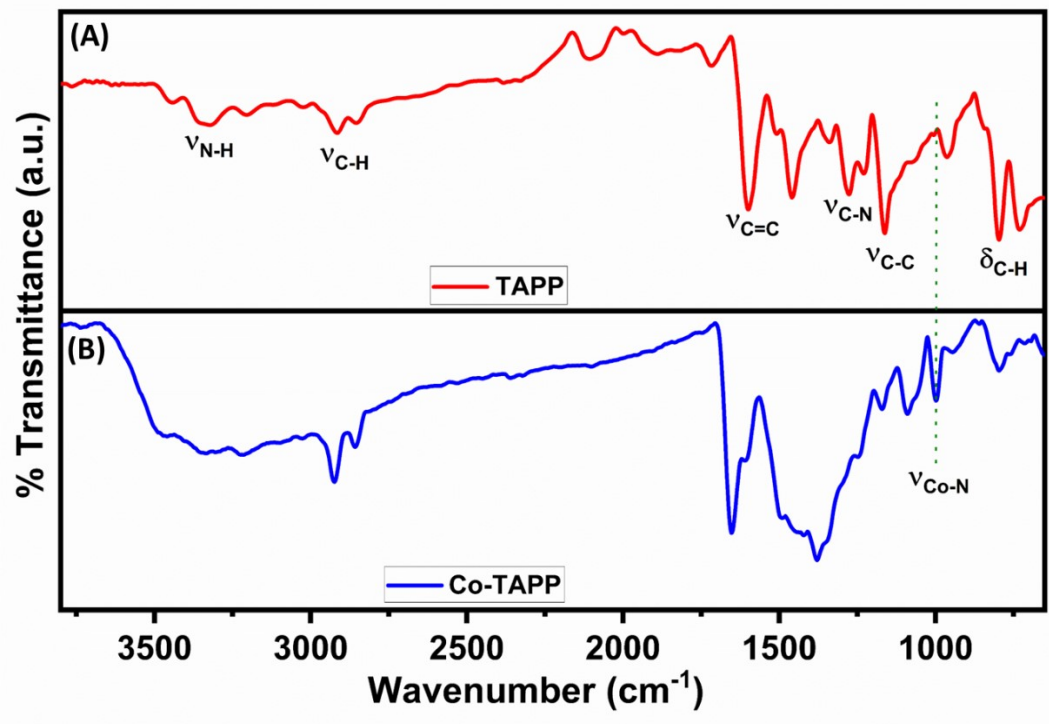


Figure S2 Comparative FTIR spectra of (A) TAPP, and (B) Co-TAPP

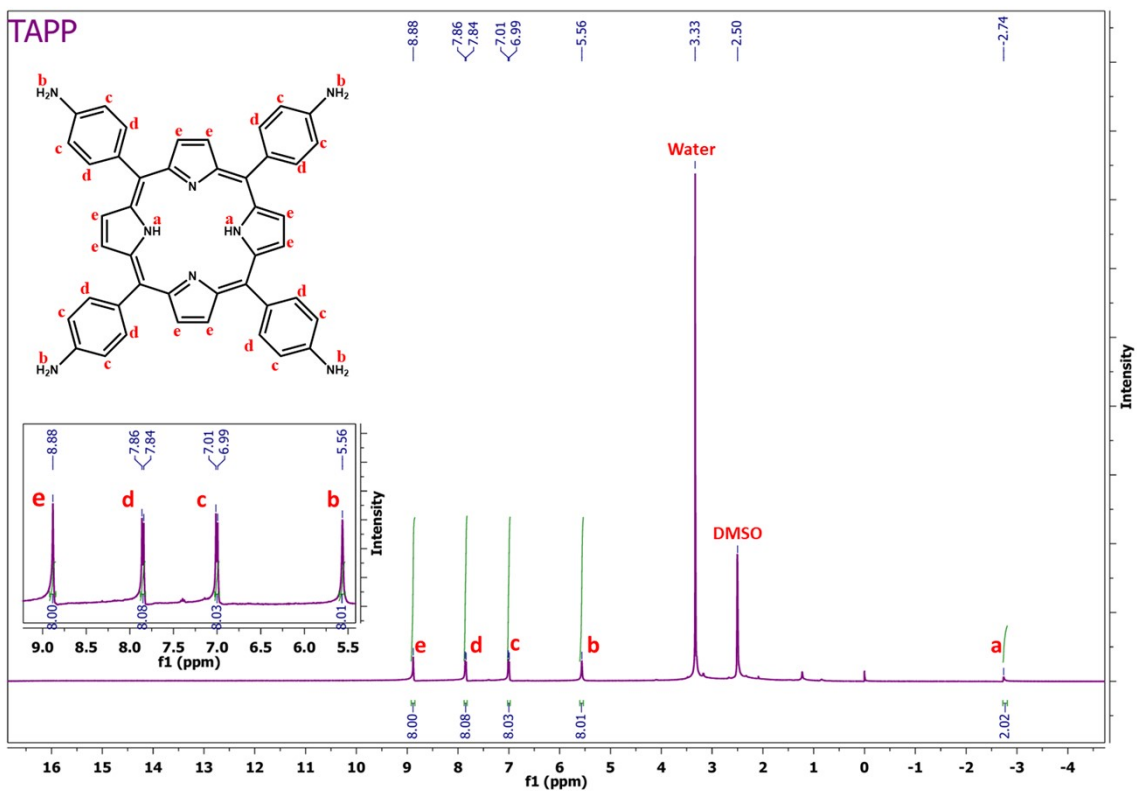


Figure S3 ^1H NMR spectrum of TAPP

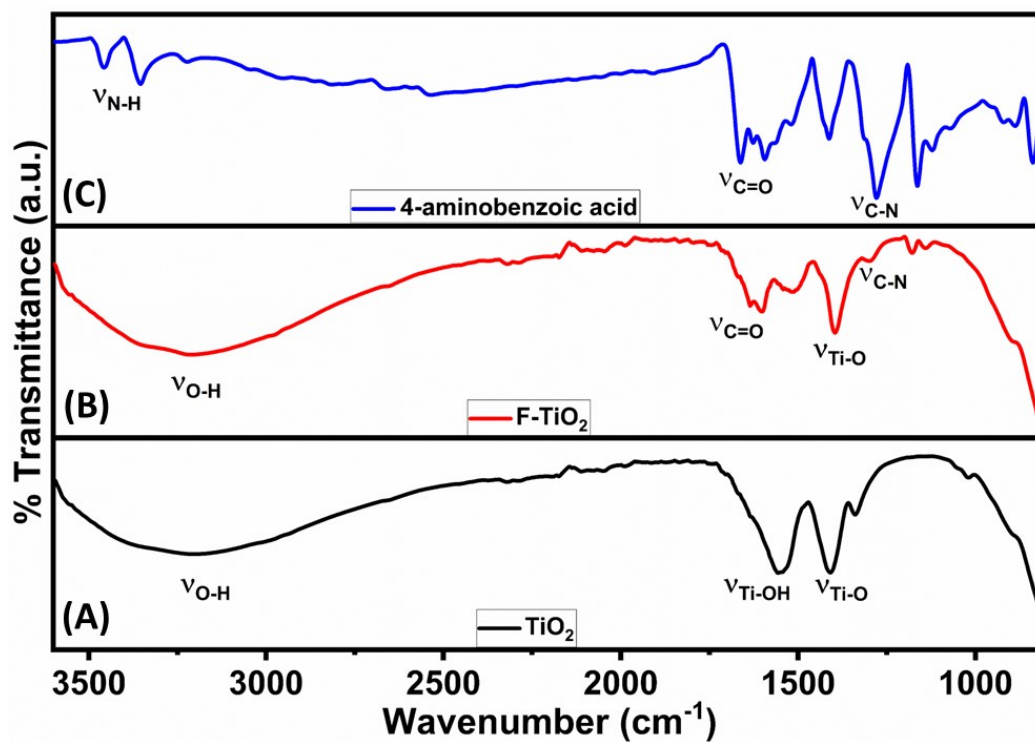


Figure S4 Comparative FTIR spectra of (A) TiO_2 , (B) Functionalized TiO_2 (F- TiO_2), and (C) 4-aminobenzoic acid

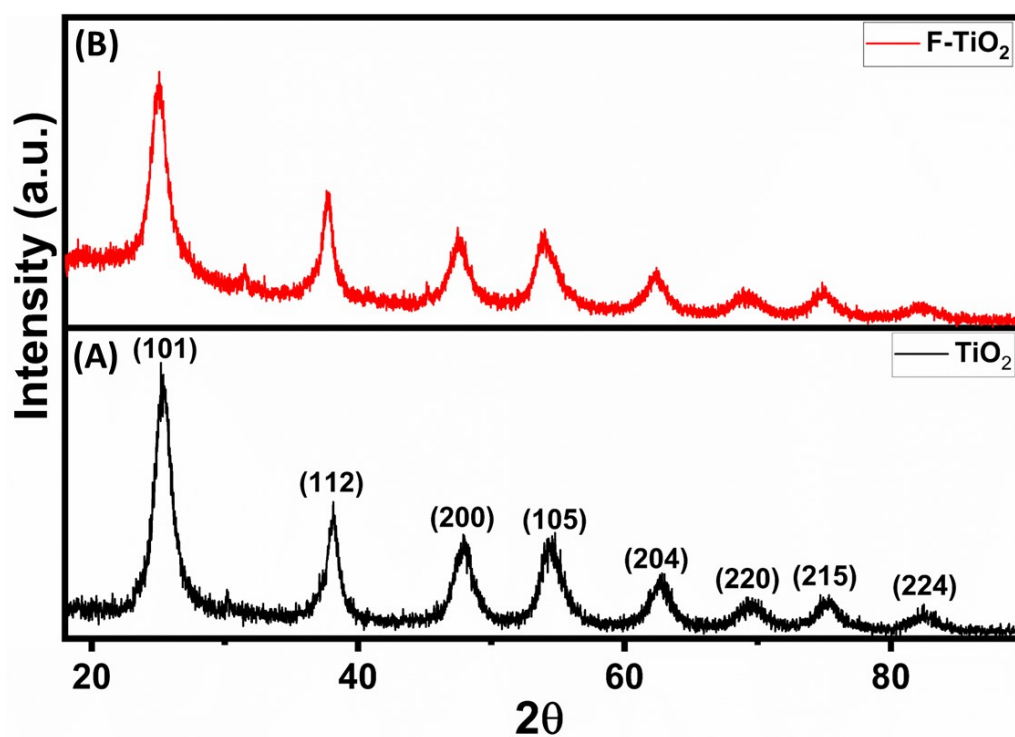


Figure S5 Powder-XRD pattern of (A) TiO_2 , and (B) F- TiO_2

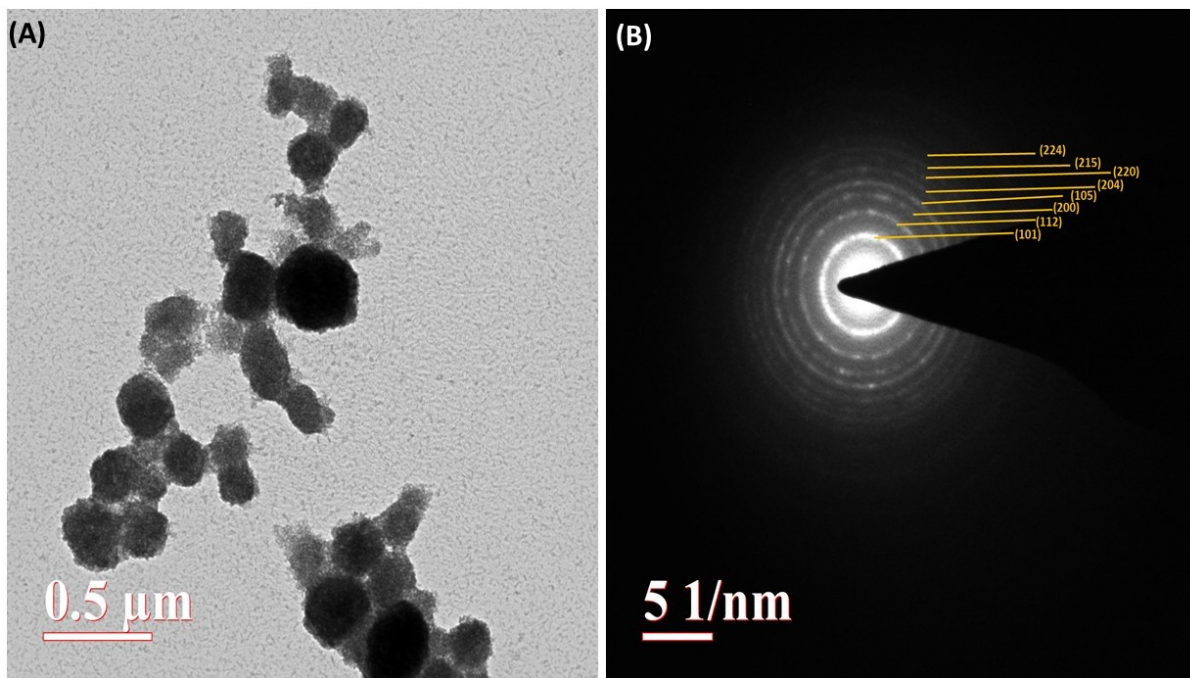


Figure S6 (A) TEM image, and (B) SAED pattern of TiO₂

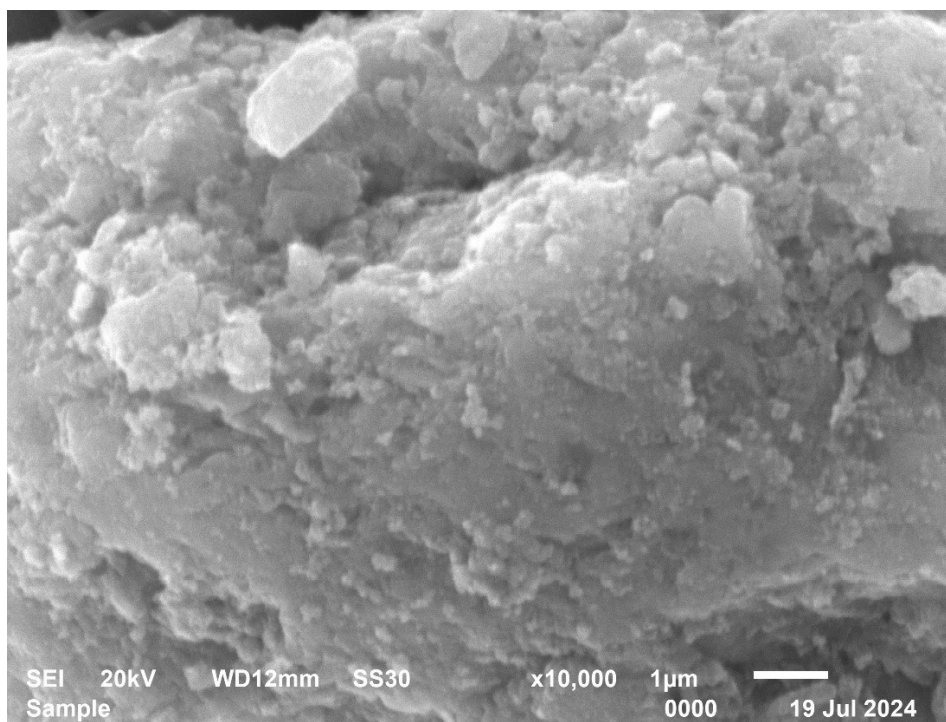


Figure S7 SEM images of F-TiO₂

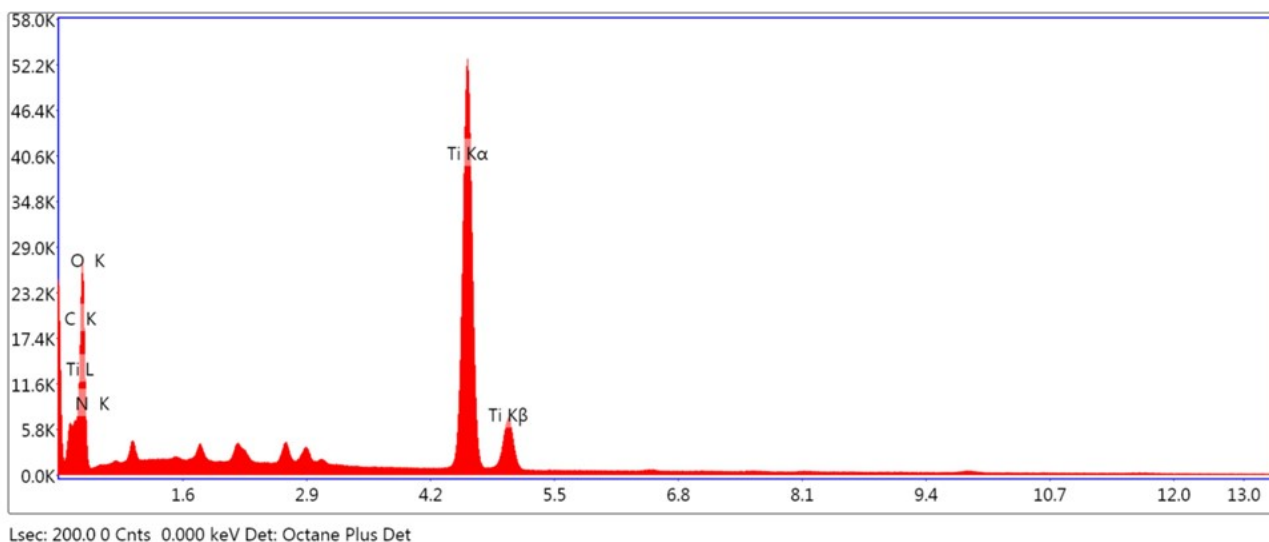


Figure S8 EDX analysis of F-TiO₂

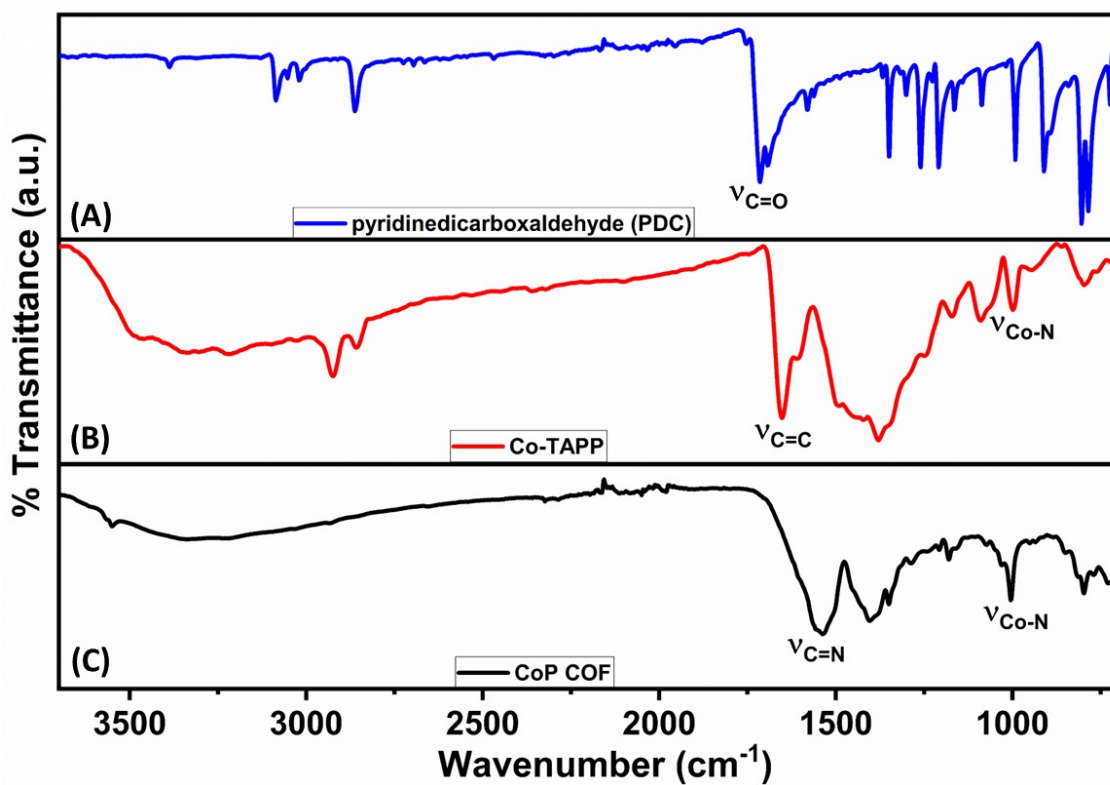


Figure S9 Comparative FTIR spectra of (A) 2,6-pyridinedicarboxaldehyde (PDC), (B) Co-TAPP, and (C) CoP COF

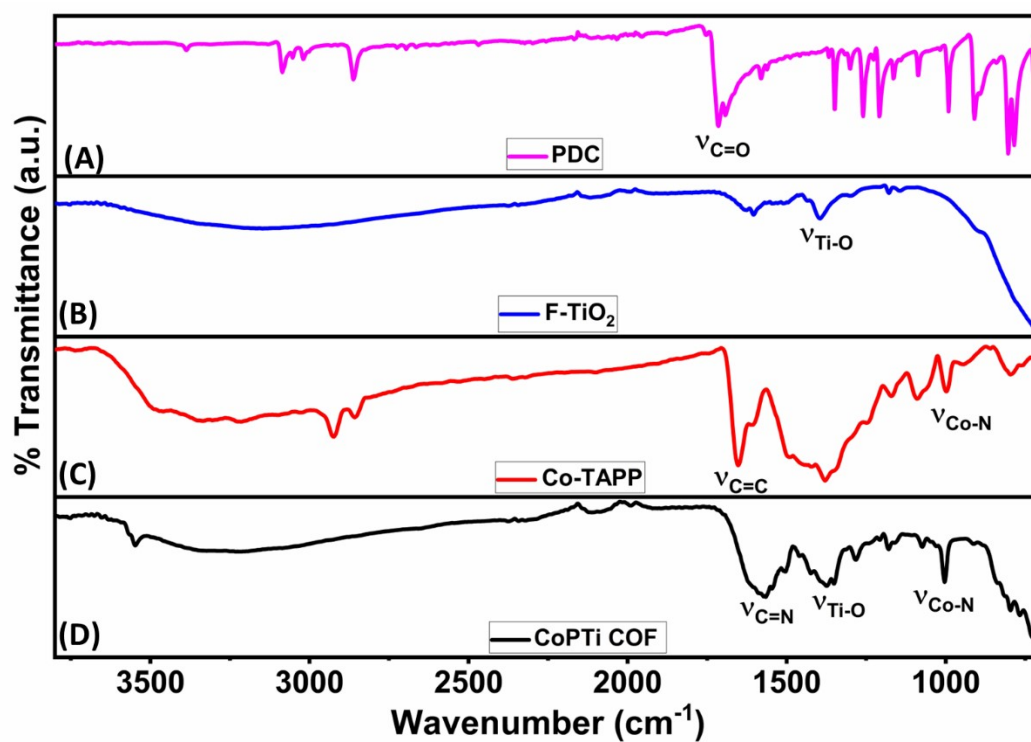


Figure S10 Comparative FTIR spectra of (A) 2,6-pyridinedicarboxaldehyde (PDC), (B) F-TiO₂, (C) Co-TAPP, and (D) CoPTi COF

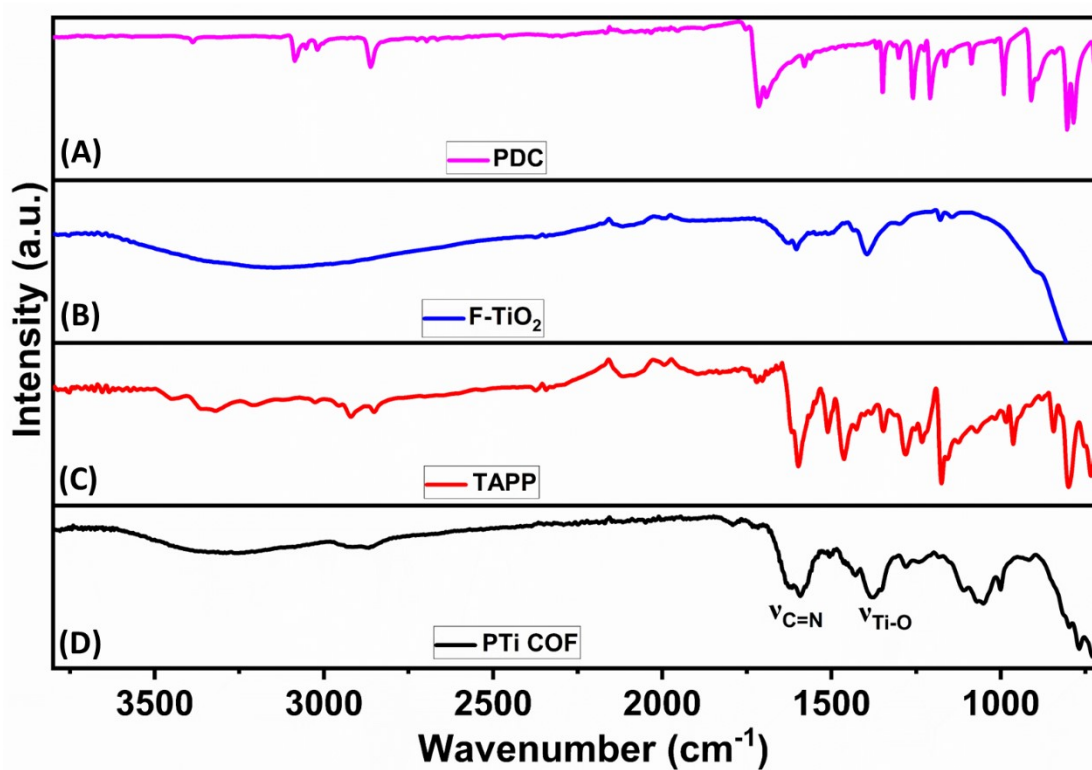


Figure S11 Comparative FTIR spectra of (A) 2,6-pyridinedicarboxaldehyde (PDC), (B) F-TiO₂, (C) TAPP, and (D) PTi COF

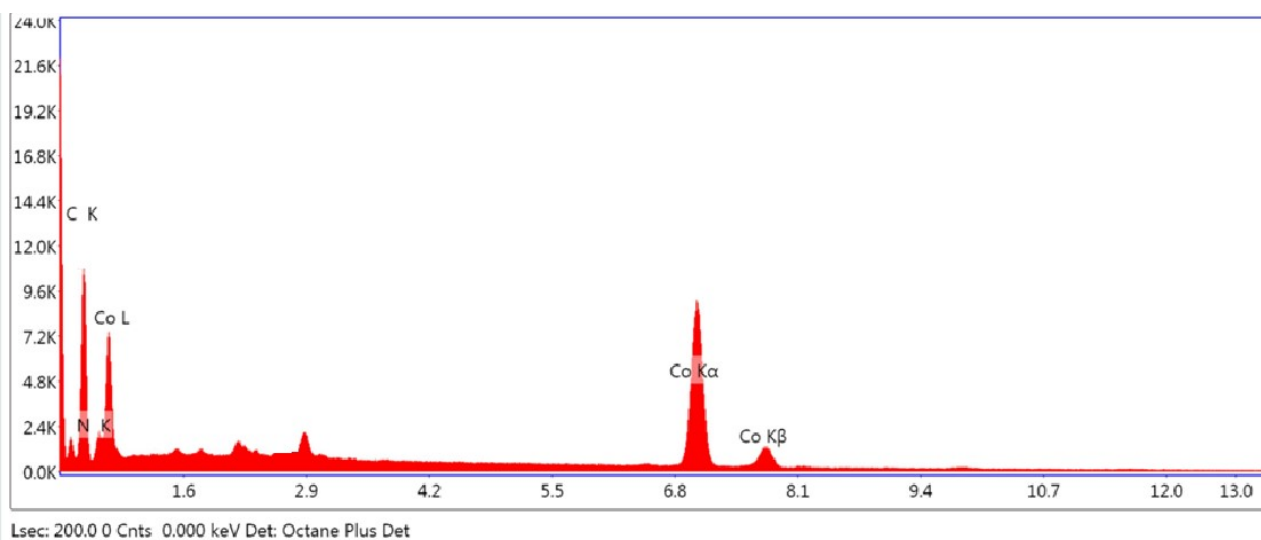


Figure S12 EDX analysis of CoP COF

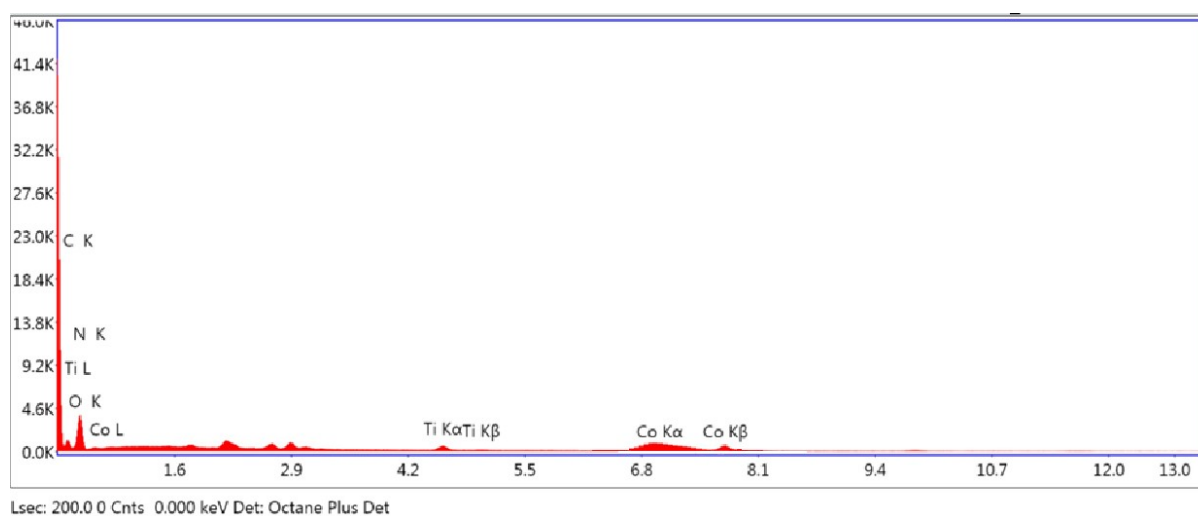


Figure S13 EDX analysis of CoPTi COF

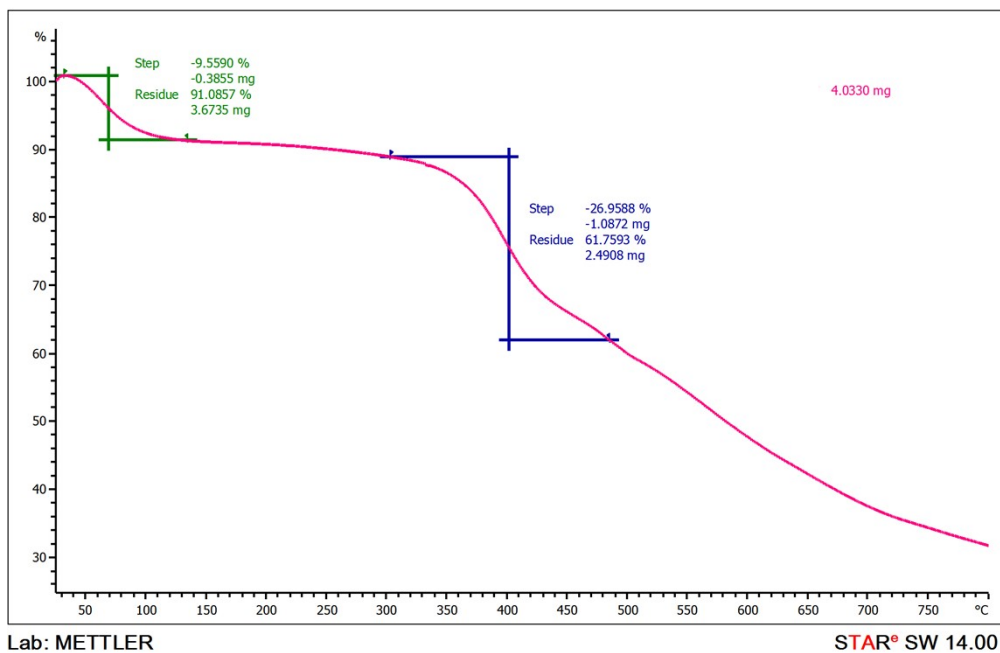


Figure S14 TGA curve of CoP COF

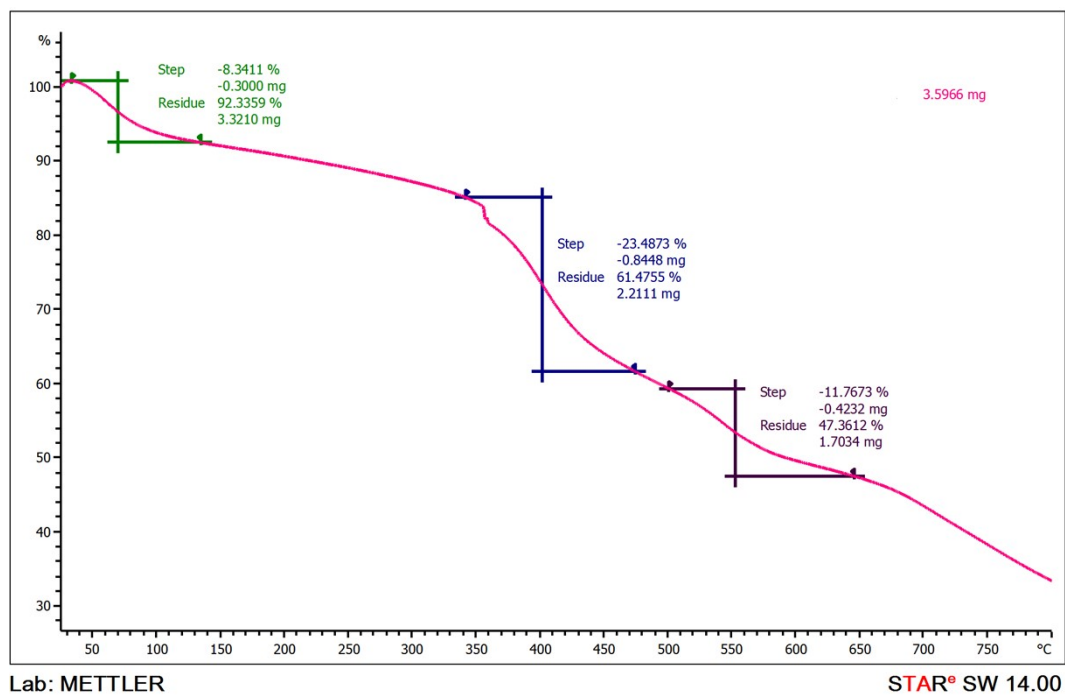


Figure S15 TGA curve of CoPTi COF

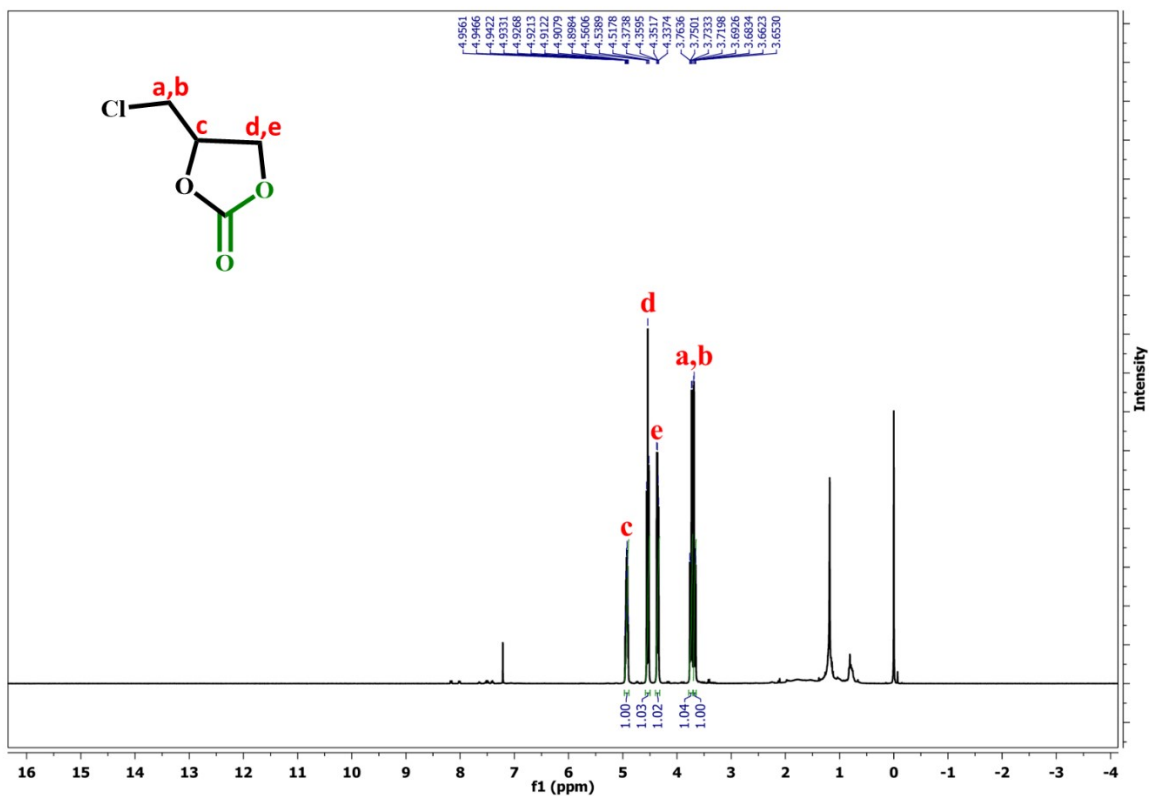


Figure S16 ^1H NMR spectrum of 4-chloromethyl-1,3-dioxolan-3-one (**1b**)

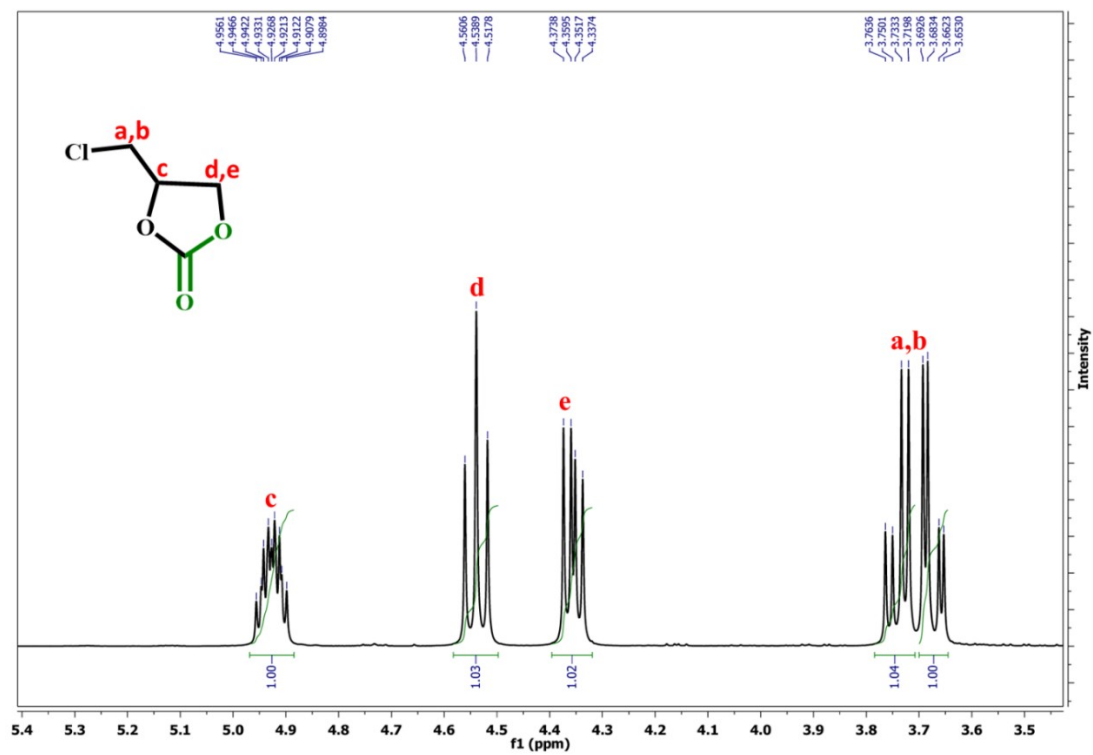


Figure S17 Magnified ^1H NMR spectrum of 4-chloromethyl-1,3-dioxolan-3-one (**1b**)

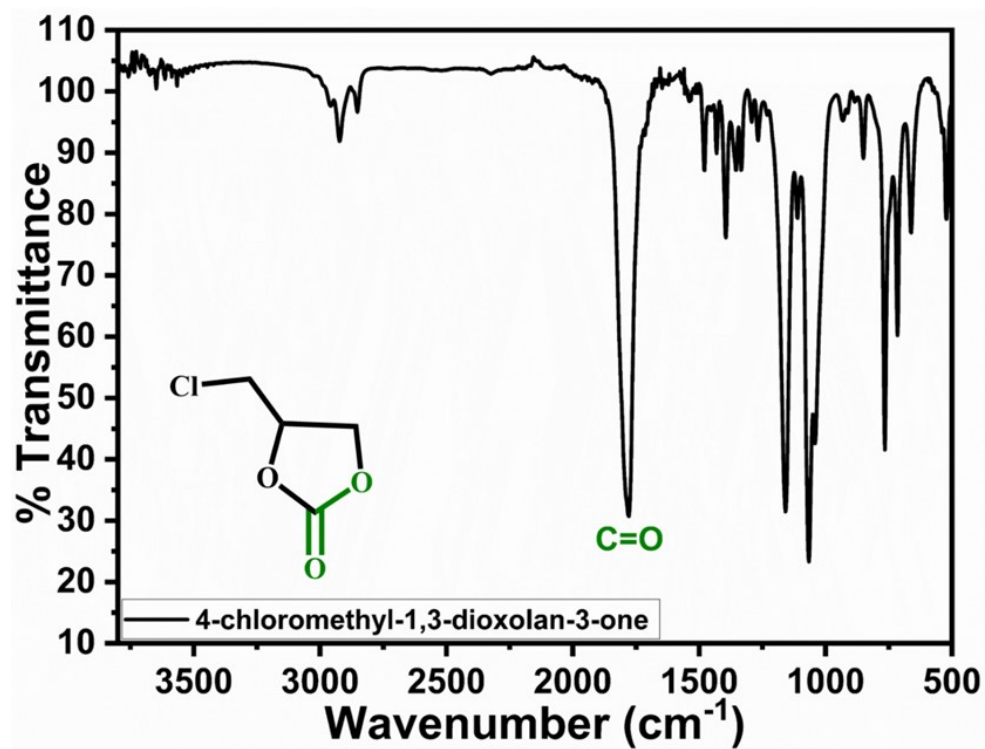


Figure S18 FTIR spectrum of 4-chloromethyl-1,3-dioxolan-3-one (**1b**)

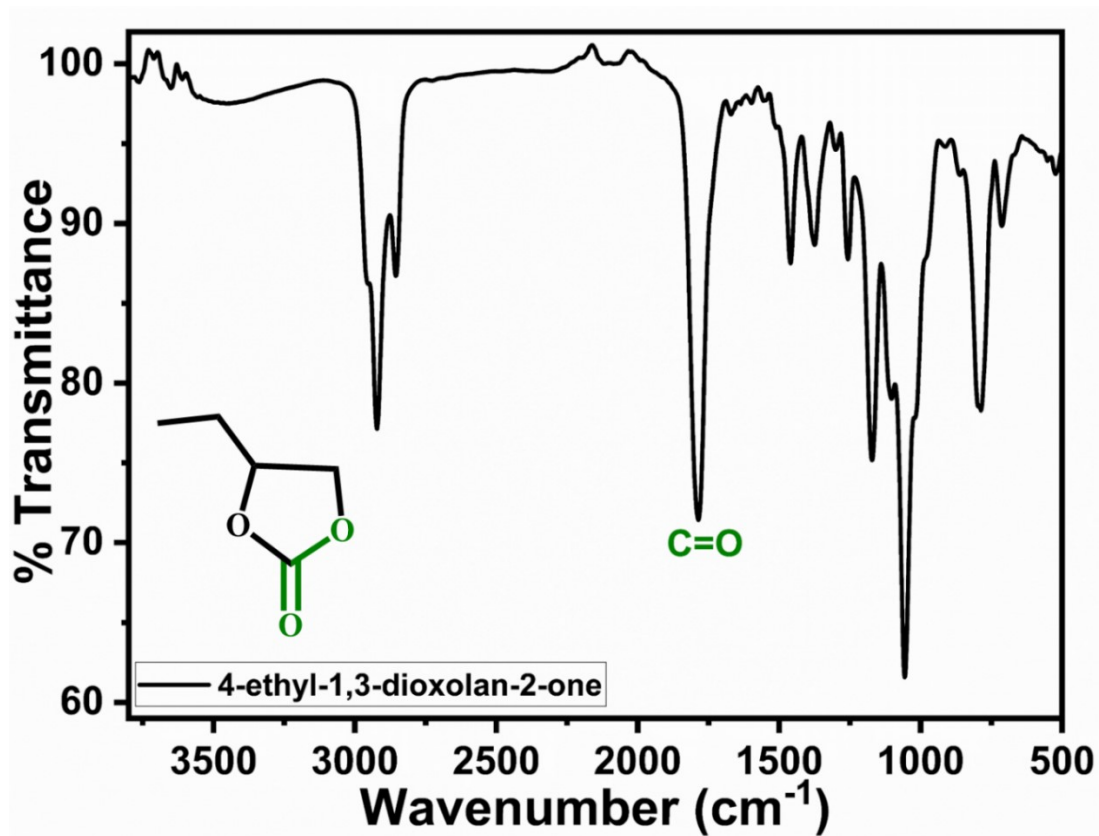


Figure S19 FTIR spectrum of 4-ethyl-1,3-dioxolan-2-one (**2b**)

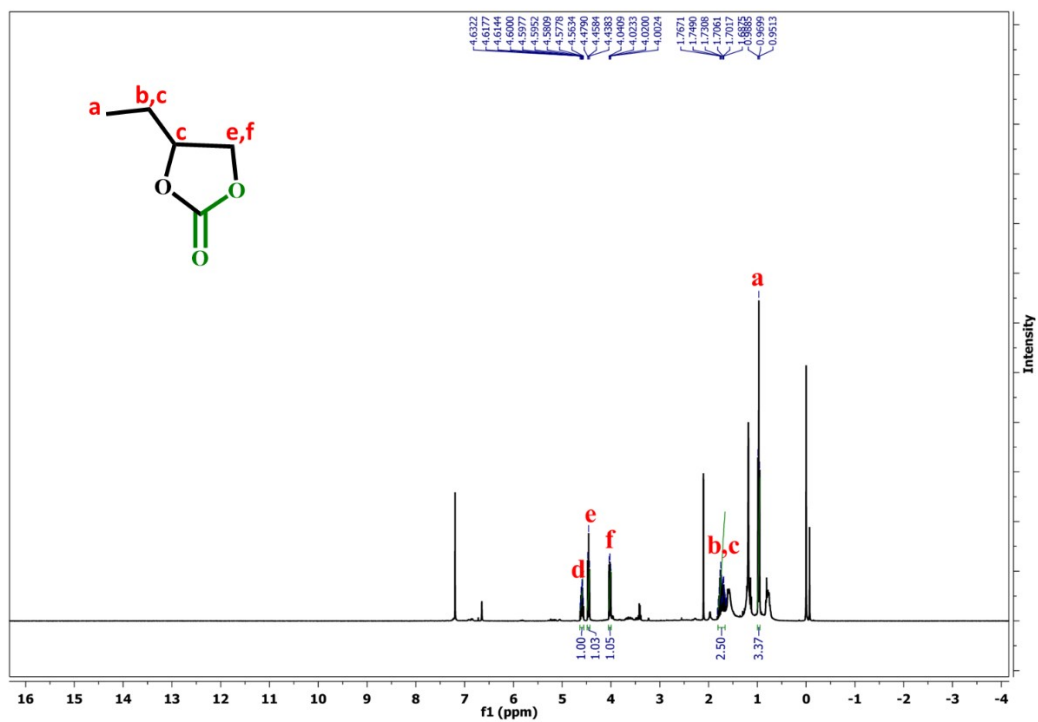


Figure S20 ^1H NMR spectrum of 4-ethyl-1,3-dioxolan-2-one (**2b**)

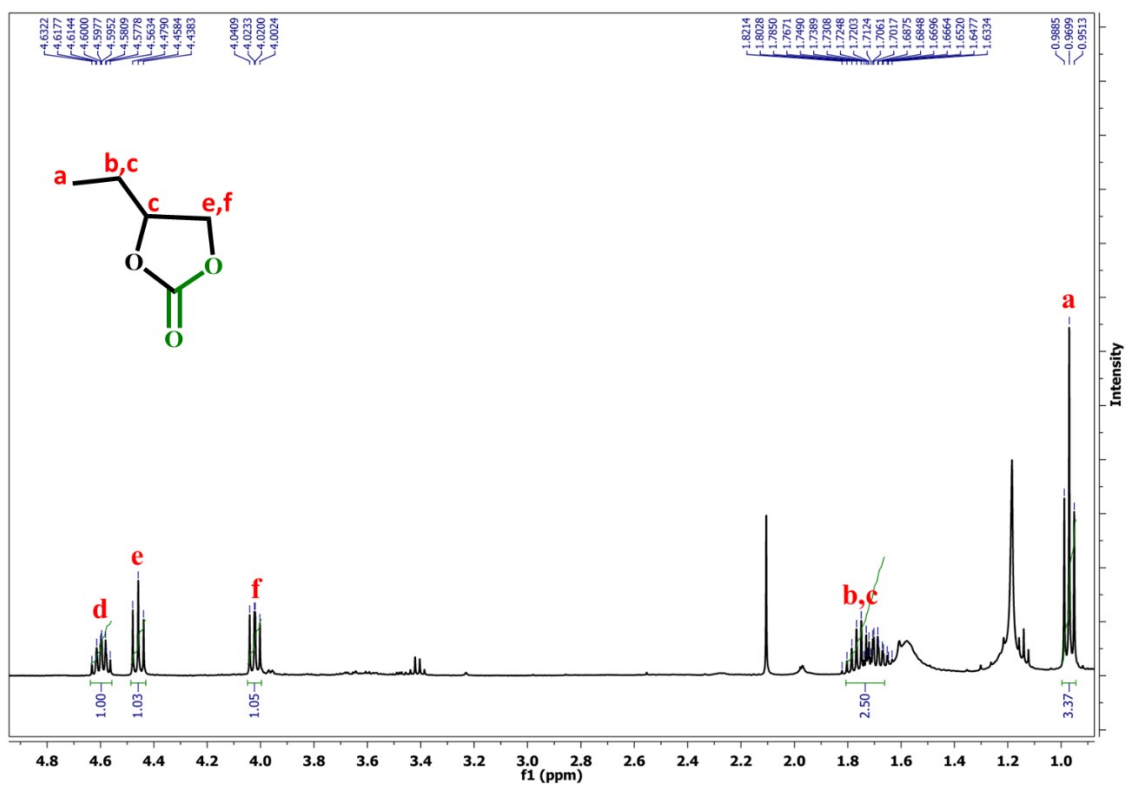


Figure S21 Magnified ^1H NMR spectrum of 4-ethyl-1,3-dioxolan-2-one (**2b**)

Fig

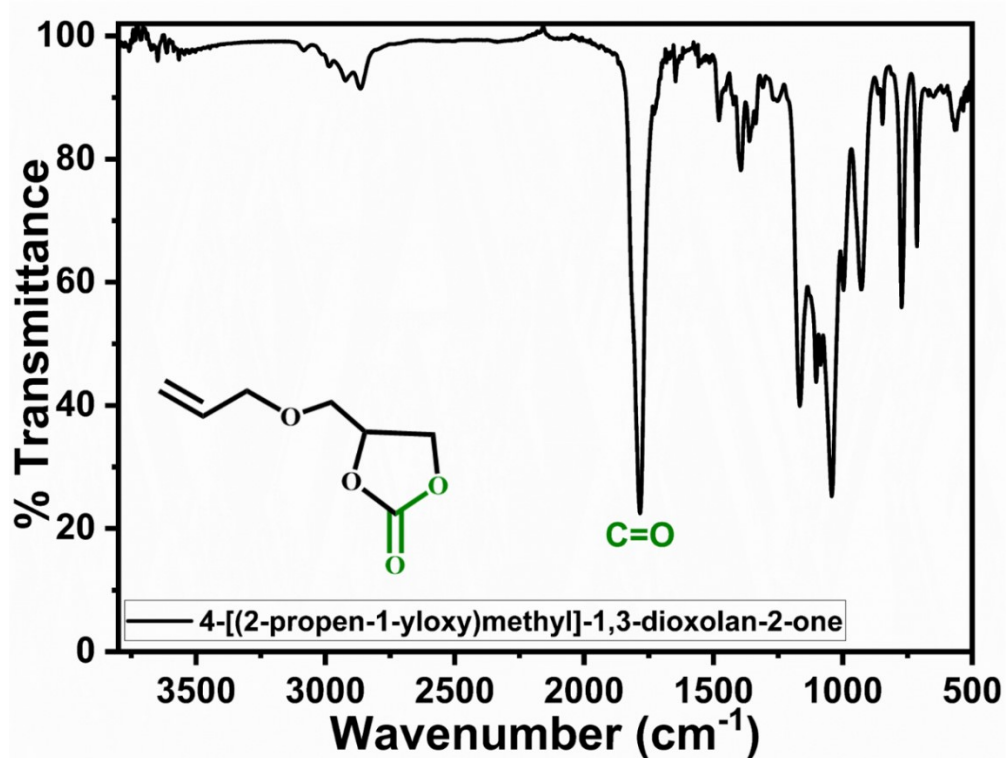


Figure S22 FTIR spectrum of 4-[(2-propen-1-yloxy)methyl]-1,3-dioxolan-2-one (**3b**)

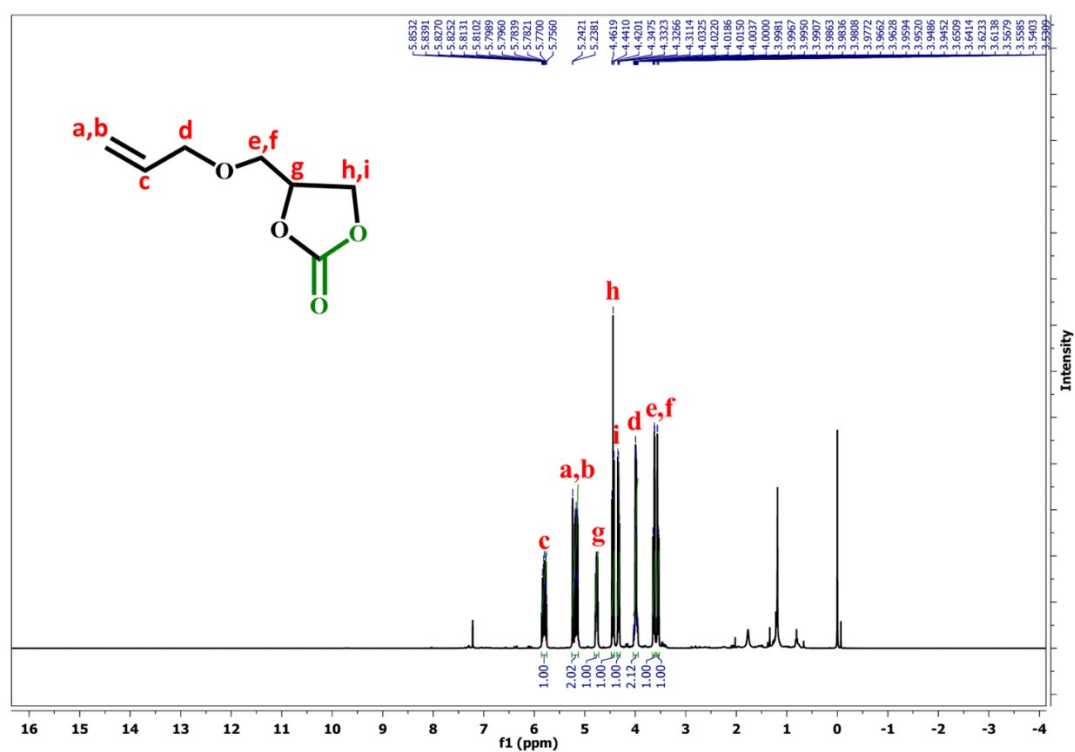


Figure S23 ^1H NMR spectrum of 4-[(2-propen-1-yloxy)methyl]-1,3-dioxolan-2-one (**3b**)

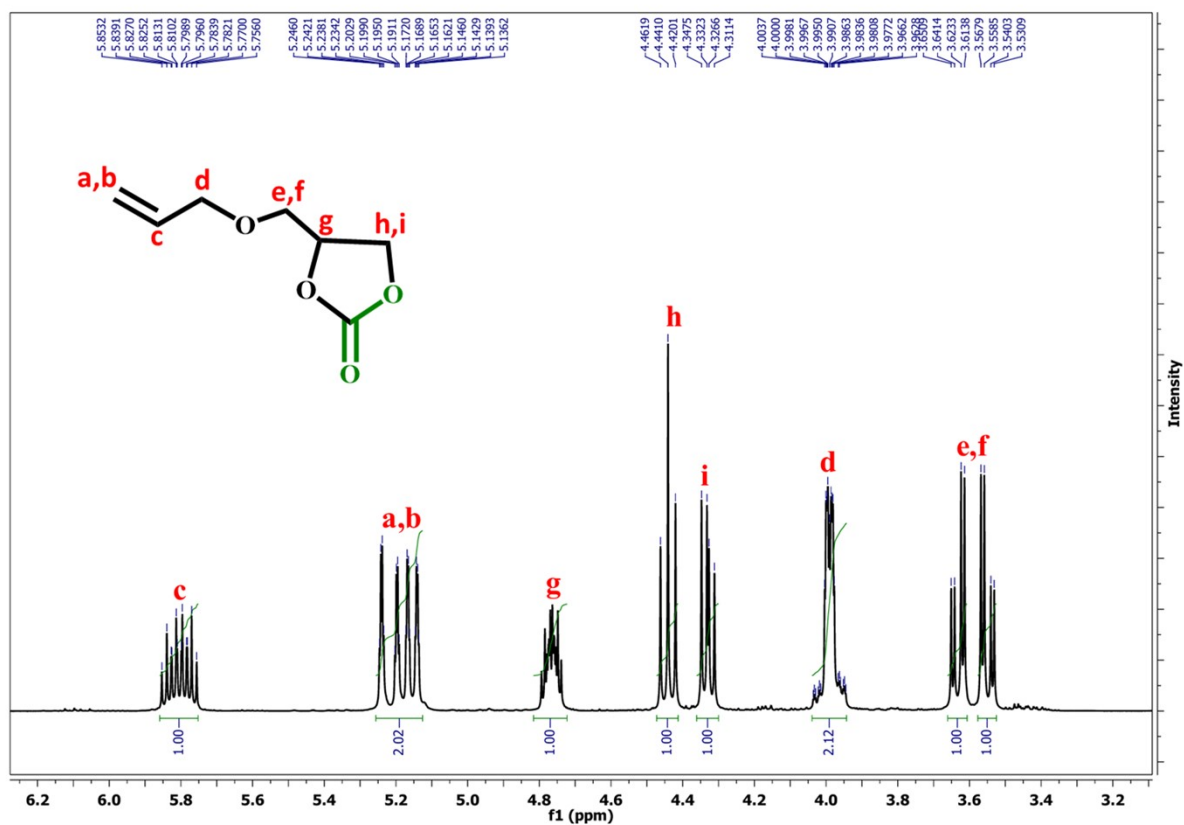


Figure S24 Magnified ^1H NMR spectrum of 4-[(2-propen-1-yloxy)methyl]-1,3-dioxolan-2-one (3b)

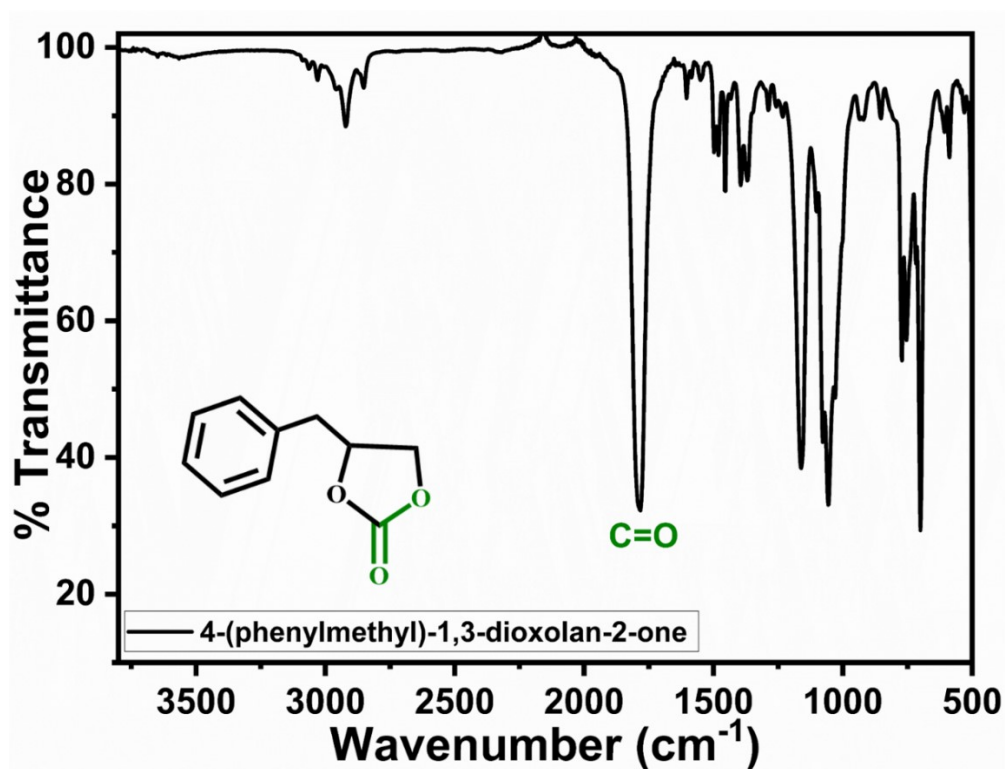
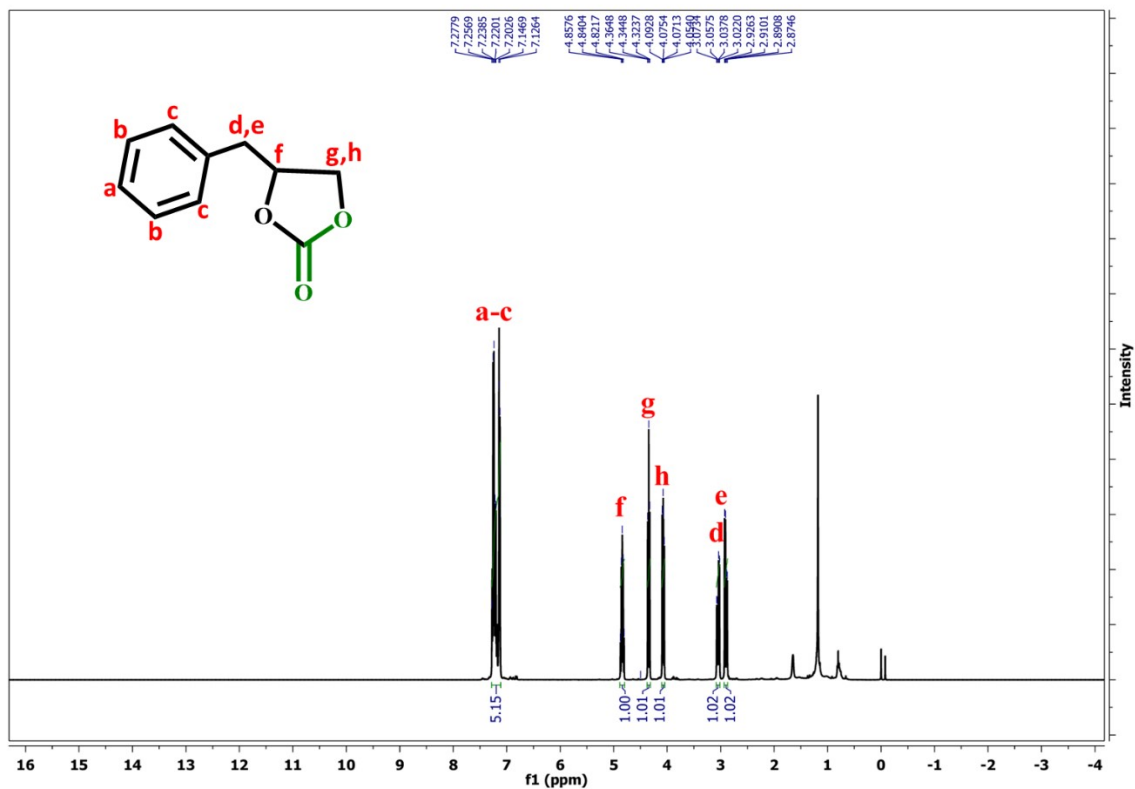


Figure S25 FTIR spectrum of 4-(phenylmethyl)-1,3-dioxolan-2-one (4b)



Fig

Figure S26 ^1H NMR spectrum of 4-(phenylmethyl)-1,3-dioxolan-2-one (4b)

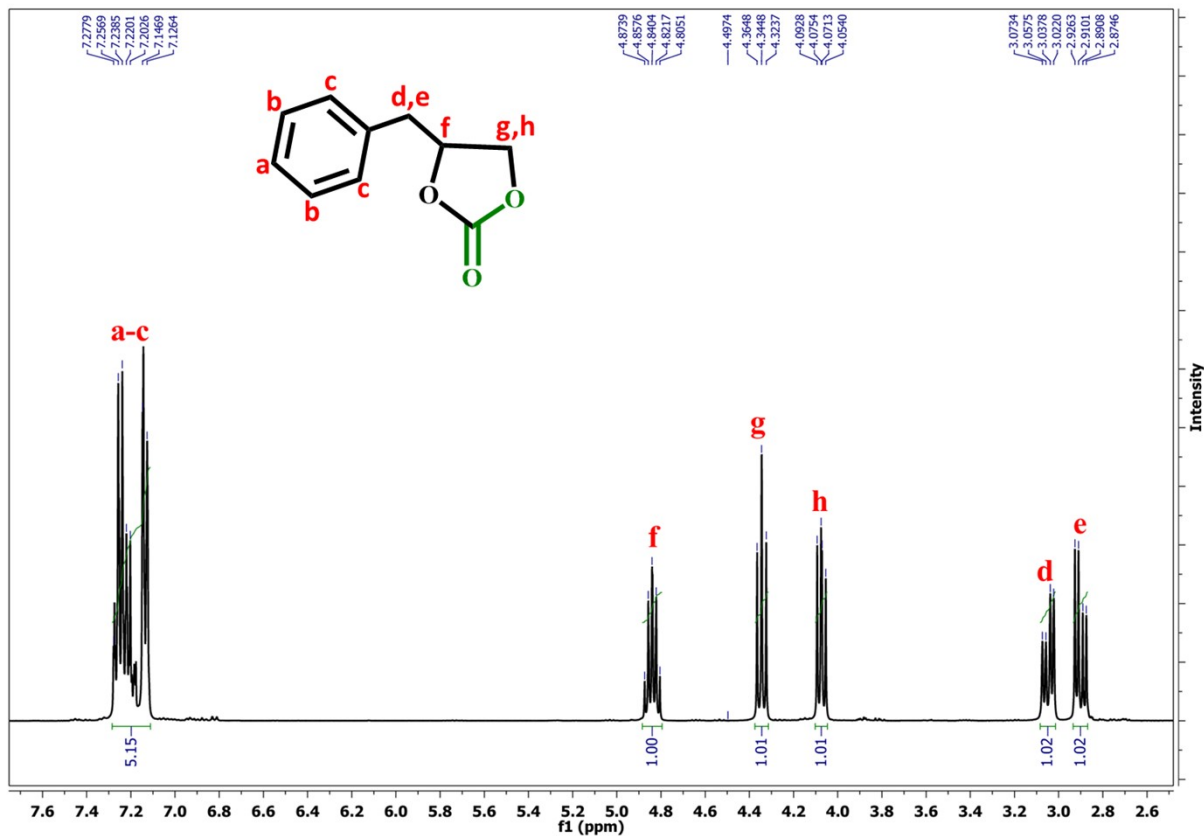


Figure S27 Magnified ^1H NMR spectrum of 4-(phenylmethyl)-1,3-dioxolan-2-one (4b)

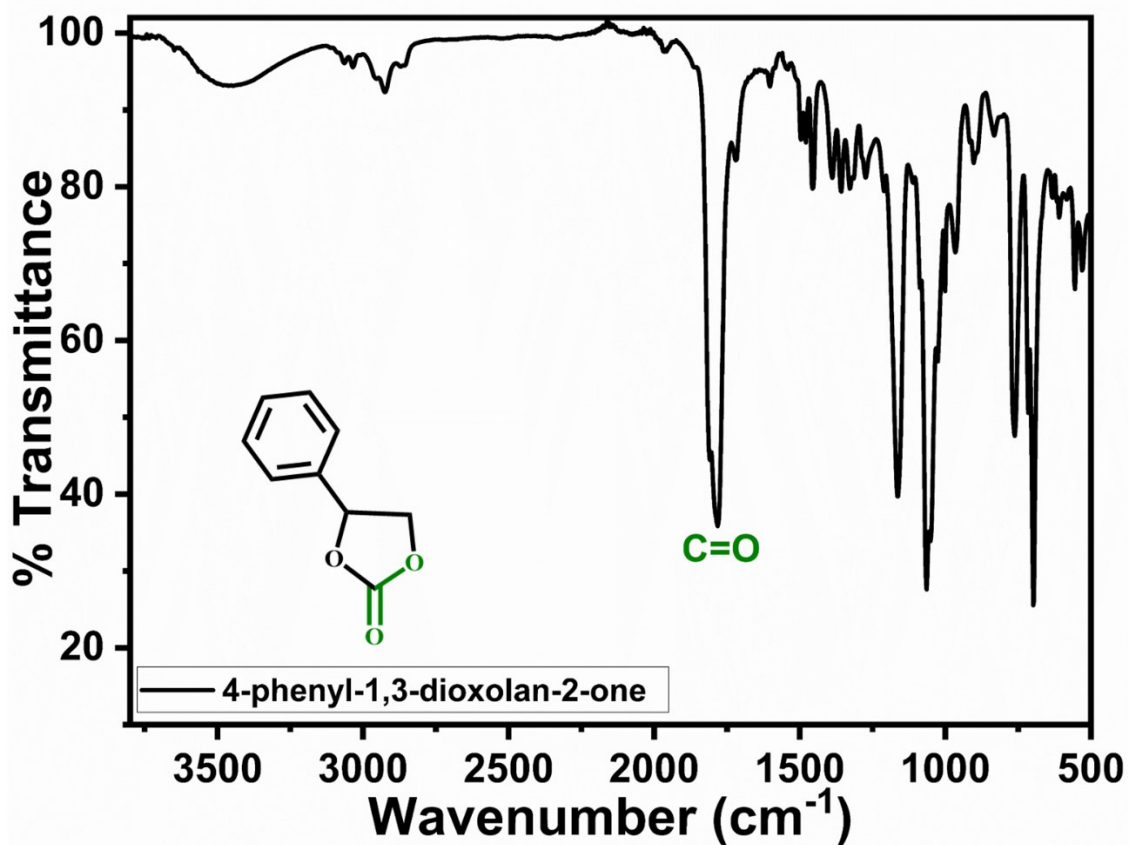


Figure S28 FTIR spectrum of 4-phenyl-1,3-dioxolan-2-one (5b)

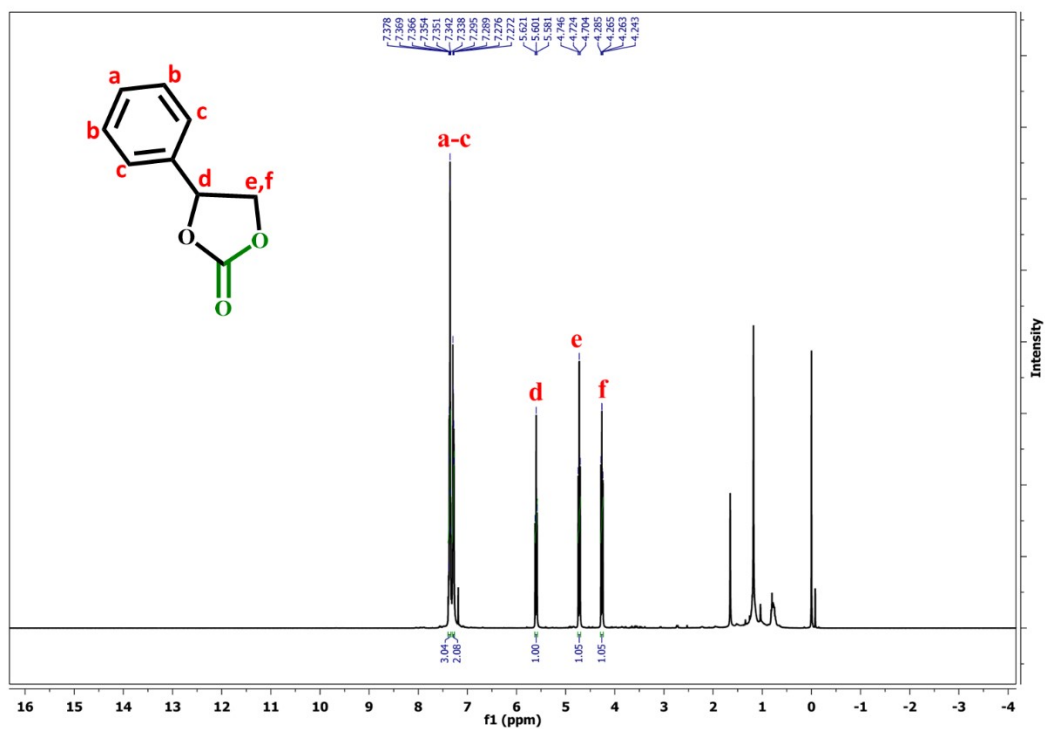


Figure S29 ¹H NMR spectrum of 4-phenyl-1,3-dioxolan-2-one (5b)

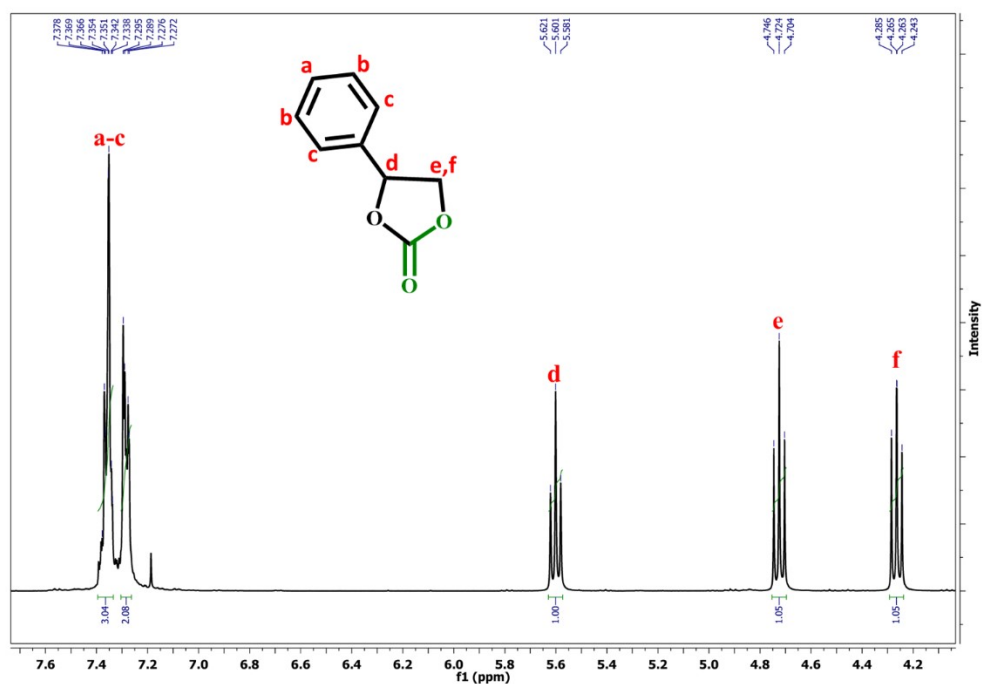


Figure S30 Magnified ^1H NMR spectrum of 4-phenyl-1,3-dioxolan-2-one (5b)

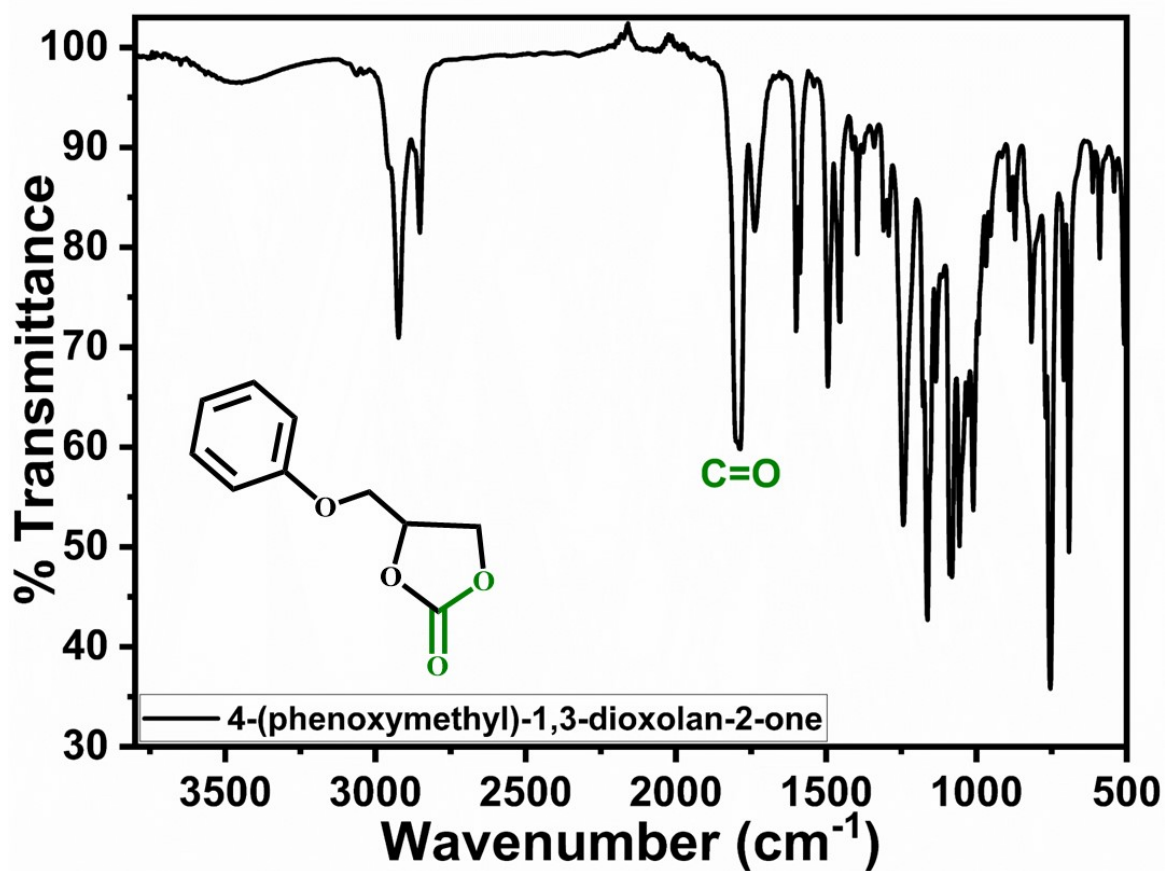


Figure S31 FTIR spectrum of 4-(phenoxy)methyl-1,3-dioxolan-2-one (6b)

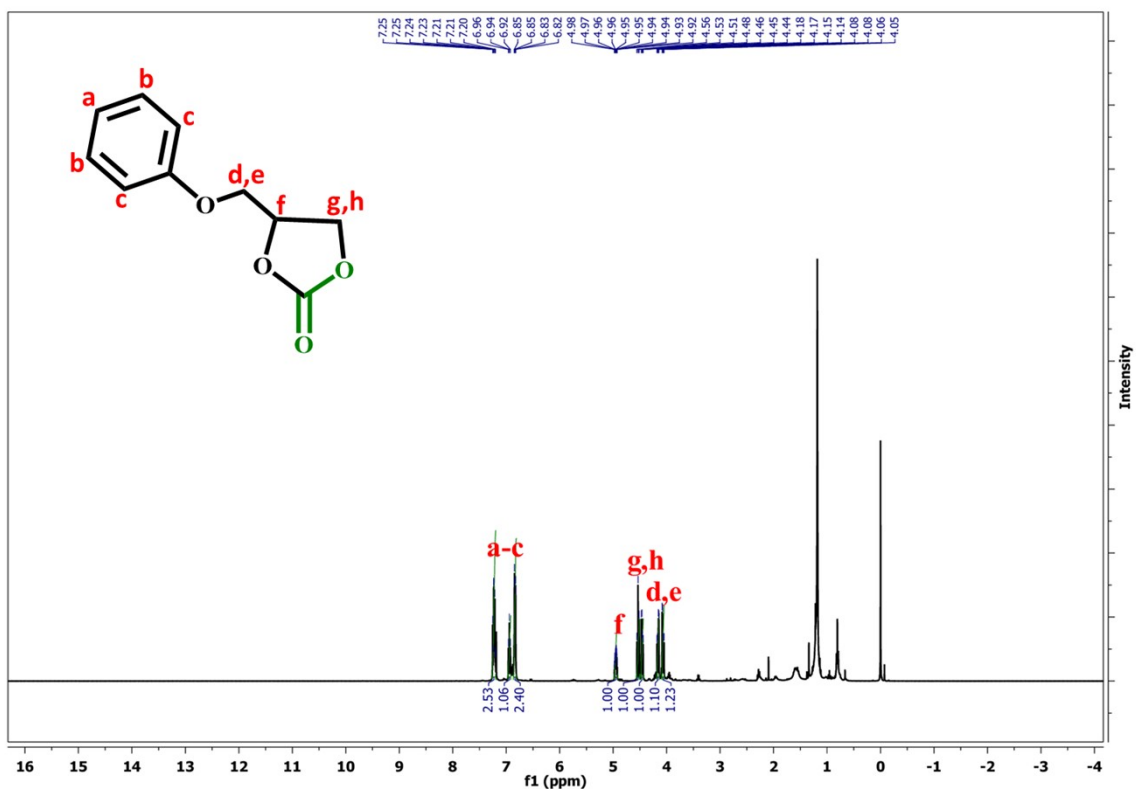


Figure S32 ^1H NMR spectrum of 4-(phenoxy)methyl-1,3-dioxolan-2-one (**6b**)

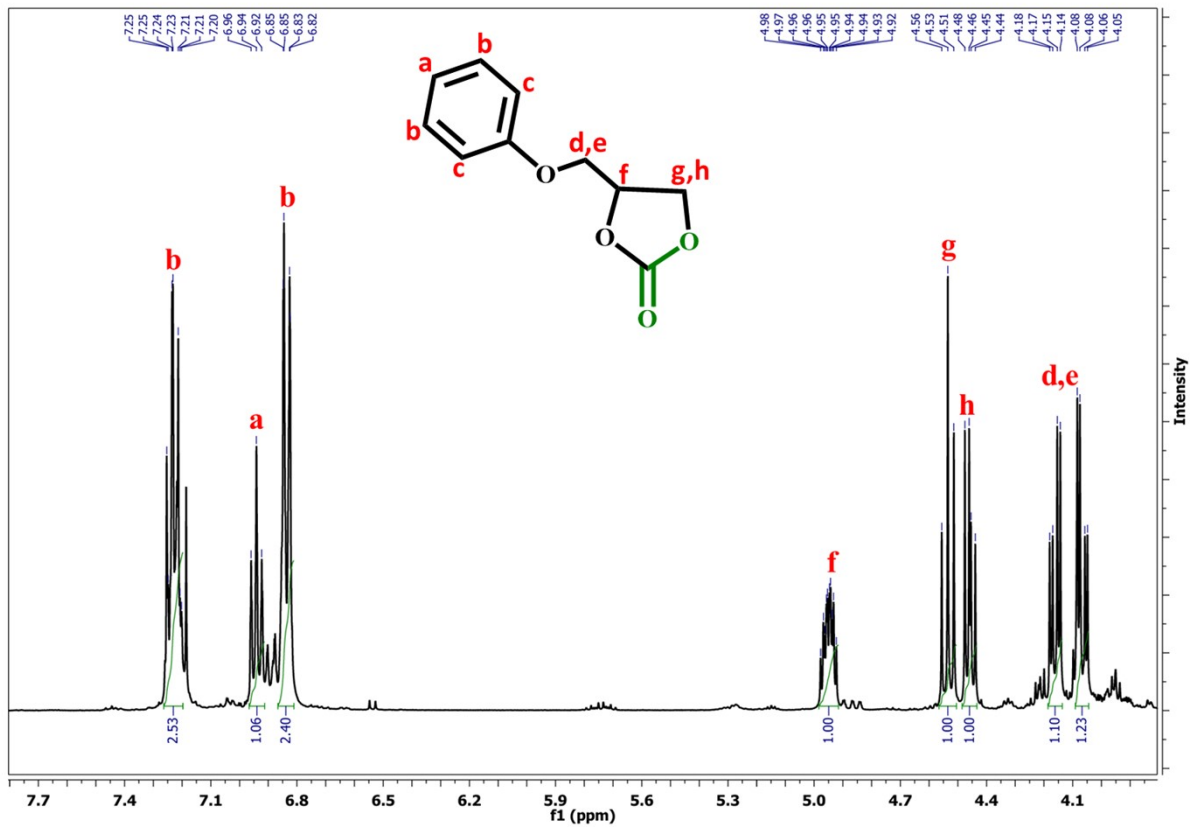


Figure S33 Magnified ^1H NMR spectrum of 4-(phenoxy)methyl-1,3-dioxolan-2-one (**6b**)

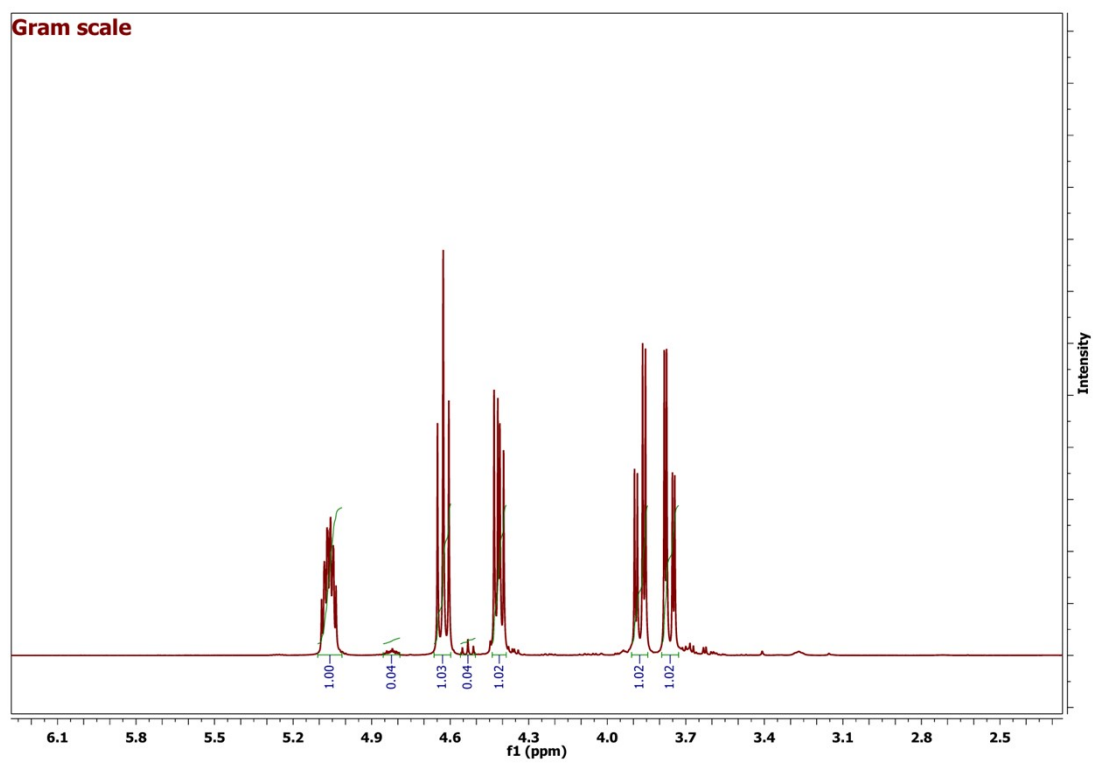


Figure S34 ^1H NMR spectrum of the product for gram scale reaction using epoxide **1a**

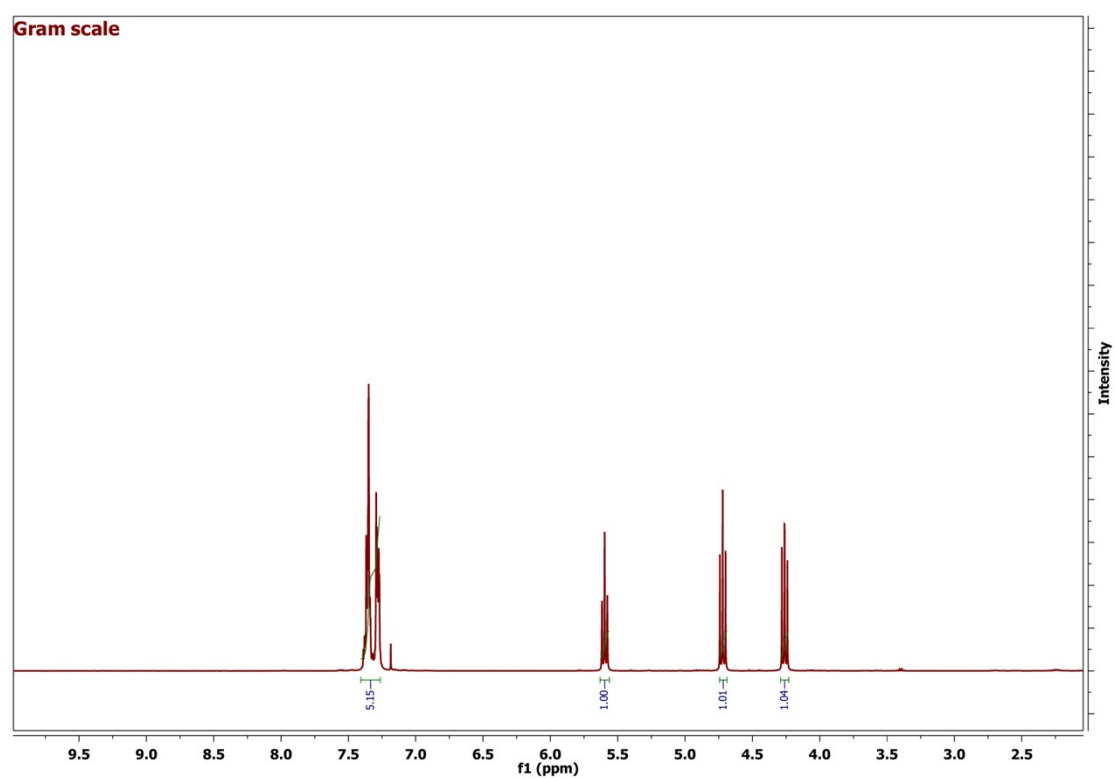


Figure S35 ^1H NMR spectrum of the product for gram scale reaction using epoxide **5a**

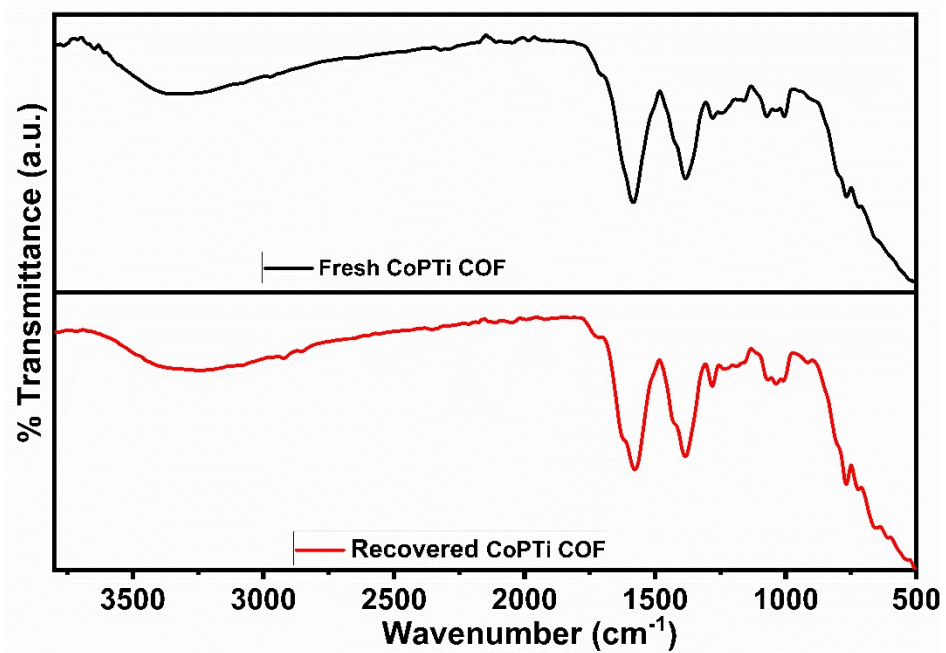


Figure S36 FTIR spectra of fresh and recovered catalyst of CoPTi COF

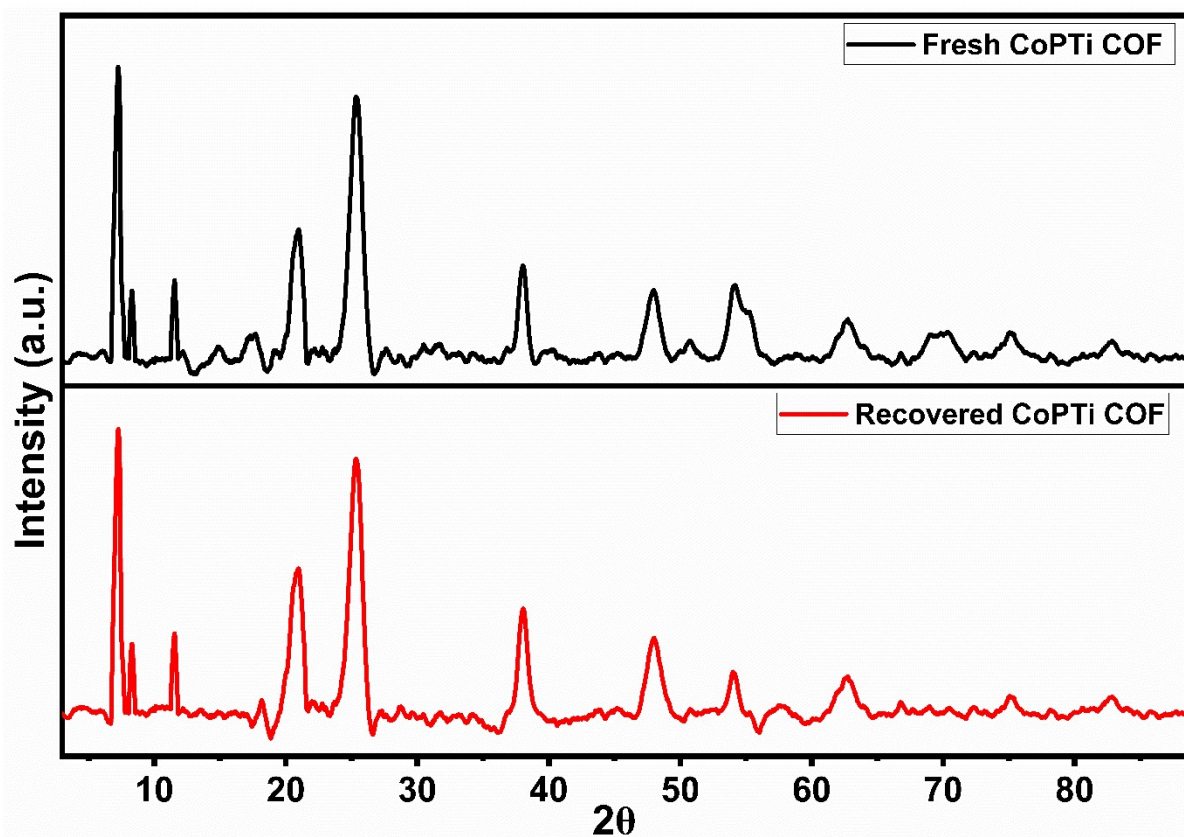


Figure S37 Powder-XRD pattern of fresh and recovered catalyst of CoPTi COF

Reference

- (1) Wang, H. M.; Jiang, J. Q.; Xiao, J. H.; Gao, R. L.; Lin, F. Y.; Liu, X. Y. Porphyrin with Amino Acid Moieties: A Tumor Photosensitizer. *Chem Biol Interact* **2008**, *172* (2), 154–158. <https://doi.org/10.1016/j.cbi.2007.11.016>.
- (2) Amiri, N.; Guergueb, M.; Al-Fakeh, M. S.; Bourguiba, M.; Nasri, H. A New Cobalt(II): Meso - Porphyrin: Synthesis, Characterization, Electric Properties and Application in the Catalytic Degradation of Dyes. *RSC Adv* **2020**, *10* (73), 44920–44932. <https://doi.org/10.1039/d0ra08786f>.
- (3) Leyva-Porras, C.; Toxqui-Teran, A.; Vega-Becerra, O.; Miki-Yoshida, M.; Rojas-Villalobos, M.; García-Guaderrama, M.; Aguilar-Martínez, J. A. Low-Temperature Synthesis and Characterization of Anatase TiO₂ Nanoparticles by an Acid Assisted Sol-Gel Method. *J Alloys Compd* **2015**, *647*, 627–636. <https://doi.org/10.1016/j.jallcom.2015.06.041>.
- (4) Wang, L.; Huang, G.; Zhang, L.; Lian, R.; Huang, J.; She, H.; Liu, C.; Wang, Q. Construction of TiO₂-Covalent Organic Framework Z-Scheme Hybrid through Coordination Bond for Photocatalytic CO₂ Conversion. *Journal of Energy Chemistry* **2022**, *64*, 85–92. <https://doi.org/10.1016/j.jechem.2021.04.053>.
- (5) Xie, Y.; Xu, M.; Wang, L.; Liang, H.; Wang, L.; Song, Y. Iron-Porphyrin-Based Covalent-Organic Frameworks for Electrochemical Sensing H₂O₂ and PH. *Materials Science and Engineering C* **2020**, *112*. <https://doi.org/10.1016/j.msec.2020.110864>.
- (6) Gao, C.-Y.; Yang, Y.; Liu, J.; Sun, Z.-M. A NiII-Cluster-Based MOF as an Efficient Heterogeneous Catalyst for the Chemical Transformation of CO₂. *Dalton Transactions* **2019**, *48* (4), 1246–1250. <https://doi.org/10.1039/C8DT04284E>.
- (7) Seong, Y.; Lee, S.; Cho, S.; Kim, Y.; Kim, Y. Organocatalysts for the Synthesis of Cyclic Carbonates under the Conditions of Ambient Temperature and Atmospheric CO₂ Pressure. *Catalysts* **2024**, *14* (1). <https://doi.org/10.3390/catal14010090>.
- (8) Carvalho Rocha, C.; Onfroy, T.; Pilmé, J.; Denicourt-Nowicki, A.; Roucoux, A.; Launay, F. Experimental and Theoretical Evidences of the Influence of Hydrogen Bonding on the Catalytic Activity of a Series of 2-Hydroxy Substituted Quaternary Ammonium Salts in the Styrene Oxide/CO₂ Coupling Reaction. *J Catal* **2016**, *333*, 29–39. <https://doi.org/10.1016/j.jcat.2015.10.014>.
- (9) Ai, J.; Min, X.; Gao, C. Y.; Tian, H. R.; Dang, S.; Sun, Z. M. A Copper-Phosphonate Network as a High-Performance Heterogeneous Catalyst for the CO₂ Cycloaddition Reactions and Alcoholysis of Epoxides. *Dalton Transactions* **2017**, *46* (20), 6756–6761. <https://doi.org/10.1039/c7dt00739f>.
- (10) Tamura, M.; Ito, K.; Honda, M.; Nakagawa, Y.; Sugimoto, H.; Tomishige, K. Direct Copolymerization of CO₂ and Diols. *Sci Rep* **2016**, *6*. <https://doi.org/10.1038/srep24038>.
- (11) Paliwal, K. S.; Patra, D.; Roy, A.; Mitra, A.; Hazarika, B. J.; Mahalingam, V. Light-Driven CO₂ Fixation into Epoxides Using an Al₂O₃/CoAl₂O₄ Composite Photocatalyst. *Inorg Chem* **2025**. <https://doi.org/10.1021/acs.inorgchem.4c04375>.

- (12) Li, T.; Xiong, J.; Chen, M.; Shi, Q.; Li, X.; Jiang, Y.; Feng, Y.; Zhang, B. A Tunable Ionic Covalent Organic Framework Platform for Efficient CO₂ Catalytic Conversion. *Front Chem Sci Eng* **2024**, *18* (1). <https://doi.org/10.1007/s11705-023-2369-x>.
- (13) Álvarez-Miguel, L.; Burgoa, J. D.; Mosquera, M. E. G.; Hamilton, A.; Whiteoak, C. J. Catalytic Formation of Cyclic Carbonates Using Gallium Aminotrisphenolate Compounds and Comparison to Their Aluminium Congeners: A Combined Experimental and Computational Study. *ChemCatChem* **2021**, *13* (19), 4099–4110. <https://doi.org/10.1002/cctc.202100910>.
- (14) Meléndez, J.; North, M.; Pasquale, R. Synthesis of Cyclic Carbonates from Atmospheric Pressure Carbon Dioxide Using Exceptionally Active Aluminium(Salen) Complexes as Catalysts. *Eur J Inorg Chem* **2007**, *2007* (21), 3323–3326. <https://doi.org/https://doi.org/10.1002/ejic.200700521>.